Excessive Balmer α Line Broadening, Power Balance, and Novel Hydride Ion Product of Plasma Formed from Incandescently Heated Hydrogen Gas with Certain Catalysts

Randell Mills, Paresh Ray, Jinquan Dong, Mark Nansteel, William Good, Peter Jansson, Bala Dhandapani, Jiliang He

BlackLight Power, Inc.

493 Old Trenton Road

Cranbury, NJ 08512

ABSTRACT

Typically the emission of vacuum ultraviolet light from hydrogen gas is achieved using discharges at high voltage, synchrotron devices, high power inductively coupled plasma generators, or a plasma is created and heated to extreme temperatures by RF coupling (e.g. $> 10^6\ K$) with confinement provided by a toroidal magnetic field. Observation of intense extreme ultraviolet (EUV) emission at low temperatures (e.g. $\approx 10^3\ K$) from atomic hydrogen generated at a tungsten filament that heated a titanium dissociator and certain gaseous atoms or ions vaporized by filament heating has been reported previously [R. Mills, J. Dong, Y. Lu, "Observation of Extreme Ultraviolet Hydrogen Emission from Incandescently Heated Hydrogen Gas with Certain Catalysts", Int. J. Hydrogen Energy, Vol. 25, (2000), pp. 919-943]. Each of the ionization of potassium, cesium, strontium, and Rb^+ and an electron transfer between two K^+ ions (K^+ / K^+) provide a reaction with a net enthalpy of an integer multiple of the potential energy of atomic hydrogen. The presence of each of the corresponding reactants formed the low applied temperature, extremely low voltage plasma called a resonance transfer or rt-plasma having strong EUV emission. Similarly, the ionization energy of Ar^+ is $27.63\ eV$, and the emission intensity of the plasma generated by atomic strontium increased significantly with the introduction of argon gas only when Ar^+ emission was observed [R. Mills, "Spectroscopic Identification of a Novel Catalytic Reaction of Atomic Hydrogen and the Hydride Ion Product", Int. J. Hydrogen Energy, Vol. 26, No. 10, (2001), pp. 1041-1058.]. In contrast, the chemically similar atoms, sodium, magnesium and barium, do not ionize at integer multiples of the potential energy of atomic hydrogen did not form a plasma and caused no emission. For further characterization, we recorded the width of the 656.2 nm Balmer α line on light emitted from rt-plasmas. Significant line broadening of 17, 9, 11, 14, *and* 24 eV was observed from a rt-plasma of hydrogen with K^+ / K^+, Rb^+, cesium, strontium, and strontium with Ar^+, respectively. These results could not be explained by Stark or thermal broadening or electric field acceleration of charged species since the measured field of the incandescent heater was extremely weak, 1 V/cm, corresponding to a broadening of much less than 1 eV. Rather the

source of the excessive line broadening is consistent with that of the observed EUV emission, an energetic reaction caused by a resonance energy transfer between hydrogen atoms and K^+/K^+, Rb^+, cesium, strontium, or Ar^+. Since line broadening is a measure of temperature, the excess power was measured calorimetrically on rt-plasmas formed by K^+/K^+ and Ar^+ as catalysts. The product hydride ion with each of K^+/K^+, Rb^+, Cs, and Ar^+ as the catalyst was predicted to have a binding energy of 3.05 eV and was observed by high resolution visible spectroscopy at 407 nm.

I. INTRODUCTION

Glow discharge devices have been developed over decades as light sources, ionization sources for mass spectroscopy, excitation sources for optical spectroscopy, and sources of ions for surface etching and chemistry [1-3]. A Grimm-type glow discharge is a well established excitation source for the analysis of conducting solid samples by optical emission spectroscopy [4-6]. Despite extensive performance characterizations, data was lacking on the plasma parameters of these devices. M. Kuraica and N. Konjevic [7] and Videnocic et al. [8] have characterized these plasma by determining the excited hydrogen atom concentrations and energies by measuring line broadening of the 656.2 nm Balmer α line. The data was analyzed in terms of Stark and Doppler effects wherein acceleration of charges such as H^+, H_2^+, and H_3^+ in the high fields (e. g. over 10 kV/cm) which were present in the cathode fall region was used to explain the Doppler component.

More recently, microhollow glow discharges have been spectroscopically studied as candidates for the development of an intense monochromatic EUV light source (e.g. Lyman α) for short wavelength lithograph for production of the next generation of integrated circuits. A neon-hydrogen microhollow cathode glow discharge has been proposed as a source of predominantly Lyman α radiation. Kurunczi, Shah, and Becker [9] observed intense emission of Lyman α and Lyman β radiation at 121.6 nm and 102.5 nm, respectively, from microhollow cathode discharges in high-pressure Ne (740 Torr) with the addition of a small amount of hydrogen (up to 3 Torr). With essentially no molecular emission observed, Kurunczi et al. attributed the anomalous Lyman α emission to the near-resonant energy transfer between the Ne_2^* excimer

and H_2 which leads to formation of $H(n=2)$ atoms, and attributed the Lyman β emission to the near-resonant energy transfer between excited Ne^* atoms (or vibrationally excited neon excimer molecules) and H_2 which leads to formation of $H(n=3)$ atoms. Despite the emission characterization of this source, data is lacking about plasma parameters.

For analyses of solids, direct current (dc) glow discharge sources have been successfully complemented by radio-frequency (rf) discharges [10]. The use of dc discharges is limited to metals; whereas, rf discharges are applicable to non-conducting materials. Other developed sources that provide a usefully intense plasma are synchrotron devices, inductively coupled plasma generators [11], and magnetically confined plasmas. Plasma characterization data on these sources is also limited.

A new plasma source has been developed that operates by incandescently heating a hydrogen dissociator to provide atomic hydrogen and heats a catalyst such that it becomes gaseous and reacts with the atomic hydrogen to produce a plasma [12-45]. It was extraordinary, that intense EUV emission was observed by Mills et al. [21-25, 31-32, 34-35] at low temperatures (e.g. $\approx 10^3\ K$) from atomic hydrogen and certain atomized elements or certain gaseous ions which singly or multiply ionize at integer multiples of the potential energy of atomic hydrogen, $27.2\ eV$ that comprise catalysts. The only pure elements that were observed to emit EUV were those wherein the ionization of t electrons from an atom to a continuum energy level is such that the sum of the ionization energies of the t electrons is approximately $m \cdot 27.2\ eV$ where t and m are each an integer.

Since Ar^+, He^+, and strontium each ionize at an integer multiple of the potential energy of atomic hydrogen, a discharge with one or more of these species present with hydrogen is anticipated to form a plasma called a resonance transfer (rt) plasma. The plasma forms by a resonance transfer mechanism involving the species providing a net enthalpy of a multiple of $27.2\ eV$ and atomic hydrogen.

Mills and Nansteel [24-25, 31] have reported that strontium atoms each ionize at an integer multiple of the potential energy of atomic hydrogen and caused emission. (The enthalpy of ionization of Sr to Sr^{5+} has a net enthalpy of reaction of $188.2\ eV$, which is equivalent to $m=7$.) The emission intensity of the plasma generated by atomic strontium

increased significantly with the introduction of argon gas only when Ar^+ emission was observed. Whereas, no emission was observed when chemically similar atoms that do not ionize at integer multiples of the potential energy of atomic hydrogen (sodium, magnesium, or barium) replaced strontium with hydrogen, hydrogen-argon mixtures, or strontium alone.

Mills and Nanstell [24-25, 31] measured the power balance of a gas cell having vaporized strontium and atomized hydrogen from pure hydrogen or argon-hydrogen mixture (77/23%) by integrating the total light output corrected for spectrometer system response and energy over the visible range. Hydrogen control cell experiments were identical except that sodium, magnesium, or barium replaced strontium. In the case of hydrogen-sodium, hydrogen-magnesium, and hydrogen-barium mixtures, 4000, 7000, and 6500 times the power of the hydrogen-strontium mixture was required, respectively, in order to achieve that same optically measured light output power. With the addition of argon to the hydrogen-strontium plasma, the power required to achieve that same optically measured light output power was reduced by a factor of about two. The power required to maintain a plasma of equivalent optical brightness with strontium atoms present was 8600 and 6300 times less than that required for argon-hydrogen and argon control, respectively. A plasma formed at a cell voltage of about 250 V for hydrogen alone and sodium-hydrogen mixtures, 140-150 V for hydrogen-magnesium and hydrogen-barium mixtures, 224 V for an argon-hydrogen mixture, and 190 V for argon alone; whereas, a plasma formed for hydrogen-strontium mixtures and argon-hydrogen-strontium mixtures at extremely low voltages of about 2 V and 6.6 V, respectively.

It was reported [23] that characteristic emission was observed from a continuum state of Ar^{2+} which confirmed the resonant nonradiative energy transfer of $27.2\ eV$ from atomic hydrogen Ar^+. The transfer of $27.2\ eV$ from atomic hydrogen to Ar^+ in the presence of a electric weak field resulted in its excitation to a continuum state. Then, the energy for the transition from essentially the Ar^{2+} state to the lowest state of Ar^+ was predicted to give a broad continuum radiation in the region of $45.6\ nm$. This broad continuum emission was observed. This emission was dramatically different from that given by an argon microwave plasma

wherein the entire Rydberg series of lines of Ar^+ was observed with a discontinuity of the series at the limit of the ionization energy of Ar^+ to Ar^{2+}. The observed Ar^+ continuum in the region of 45.6 nm confirmed the rt-plasma mechanism of the excessively bright, extraordinarily low voltage discharge. The product hydride ion with Ar^+ as a reactant was predicted to have a binding energy of 3.05 eV and was observed spectroscopically at 407 nm [23].

He^+ ionizes at 54.417 eV which is $2 \cdot 27.2\ eV$, and novel EUV emission lines were observed from microwave and glow discharges of helium with 2% hydrogen [18-19, 27]. The observed energies were $q \cdot 13.6\ eV$ ($q = 1,2,3,4,6,7,8,9,$ *or* 11) or these energies less 21.2 eV due to inelastic scattering of the lines by helium atoms in the excitation of $He\,(1s^2)$ to $He\,(1s^1 2p^1)$. These lines can be explained by the resonance transfer of $m \cdot 27.2\ eV$.

The plasma parameters of rt-plasmas were previously studied by EUV spectroscopy [18-25, 31-35], characteristic emission from catalysis and the hydride ion products [21-23], lower-energy hydrogen emission [16, 18-20], plasma formation [21-25, 31-32, 34-35], Balmer α line broadening [19, 28-29], elevated electron temperature [19, 28], anomalous plasma afterglow duration [34-35], power generation [24-31, 42], and analysis of chemical compounds [36-42]. To further characterize these plasmas, the width of the 656.2 nm Balmer α line was recorded on light emitted from rt-plasmas formed from hydrogen with K^+/K^+, Rb^+, Cs, Sr, or Ar^+. Since line broadening is a measure of temperature, the power balance of rt-plasmas formed with K^+/K^+ and $Sr-Ar^+$ catalysts were measured calorimetrically. The product hydride ion with each of K^+/K^+, Rb^+, Cs, and Ar^+ as the catalyst was predicted to have a binding energy of 3.05 eV corresponding to emission at 407 nm. Thus, the high resolution visible spectra covering the region of 407 nm was recorded.

II. EXPERIMENTAL

A. Balmer line broadening and high resolution visible spectroscopy recorded on rt-plasmas

The width of the 656.2 nm Balmer α line was recorded on light

emitted from a hydrogen glow discharge performed according to methods reported previously [29] that served as a control for measurements recorded on light emitted from rt-plasmas of hydrogen with K_2CO_3, KNO_3, $RbNO_3$, Cs_2CO_3, strontium or strontium with an argon-hydrogen mixture (97/3%). The experimental set up shown in Figure 1 comprised a quartz cell which was 500 mm in length and 50 mm in diameter. The entire quartz cell was enclosed in an Alumina insulation package. Several K-type thermocouples were located in the insulation. The thermocouples were monitored with a multichannel computer data acquisition system. A Pyrex cap sealed to the quartz cell with a Viton O ring and a C-clamp incorporated ports for gas inlet, outlet, and photon detection. A tungsten filament (0.508 mm in diameter and 800 cm in length, total resistance ~2.5 ohm) heater and hydrogen dissociator were in the quartz tube as well as a cylindrical titanium screen (300 mm long and 40 mm in diameter) that served as a second hydrogen dissociator in the case of experiments with carbonates and nitrates. The filament was coiled on a grooved ceramic tube support to maintain its shape when heated. The return lead passed through the inside of the ceramic tube. The inorganic test materials were coated on a titanium screen dissociator by the method of wet impregnation. The screen was coated by dipping it in a 0.6 M K_2CO_3/10% H_2O_2, 0.6 M KNO_3/10% H_2O_2, 0.6 M $RbNO_3$/10% H_2O_2, 0.6 M Cs_2CO_3/10% H_2O_2, or 0.6 M $SrCO_3$/10% H_2O_2, and the crystalline material was dried on the surface by heating for 12 hours in a drying oven at 130 °C. A new dissociator was used for each experiment. The titanium screen was electrically floated with power applied to the filament. In a repeat of the rt-plasma formed with strontium, the titanium screen was removed, and about 1 g of strontium metal (Alfa Aesar 99.95%) was placed in the center of the cell under one atmosphere of dry argon in a glovebox. The cell was sealed, removed from the glovebox, and connected to an EUV spectrometer. Strontium was vaporized by the filament heater. In each test, power was applied to the filament by a DC power supply which was controlled by a constant power controller. The power applied to the filament was 300 W. The voltage across the filament was about 55 V and the current was about 5.5 A at 300 W. The temperature of the tungsten filament was estimated to be in the range 1100 to 1500 °C. The external cell wall temperature was about 700 °C.

The cell was operated under gas flow conditions while maintaining a constant gas pressure in the cell. Each gas was ultrahigh purity. The gas pressure inside the cell was maintained at about 300 mtorr with a hydrogen flow rate of 5.5 sccm or an argon flow rate of 5.2 sccm and a hydrogen flow rate of 0.3 sccm. Each gas flow was controlled by a 0-20 sccm range mass flow controller (MKS 1179A21CS1BB) with a readout (MKS type 246). The cell pressure was monitored by a 0-10 torr MKS Baratron absolute pressure gauge.

The light emission was introduced to an EUV spectrometer for spectral measurement. The spectrometer was a McPherson 0.2 meter monochromator (Model 302, Seya-Namioka type) equipped with a 1200 lines/mm holographic grating with a platinum coating. The wavelength region covered by the monochromator was $30-560\,nm$. A channel electron multiplier (CEM) was used to detect the EUV light. The wavelength resolution was about $1\,nm$ (FWHM) with an entrance and exit slit width of $300\,\mu m$. The vacuum inside the monochromator was maintained below $5X10^{-4}$ Torr by a turbo pump. The Lyman α emission was recorded as a function of time after the filament was turned on. In each case, the EUV spectrum ($40-160\,nm$) of the rt-plasma cell emission was recorded at about the point of the maximum Lyman α emission to confirm the rt-plasma before the line broadening and high resolution visible spectrum in the region of $407\,nm$ were recorded.

The plasma emission from the hydrogen glow discharge and each rt-plasma maintained in the filament heated cell was fiber-optically coupled through a 220F matching fiber adapter positioned 2 cm from the sapphire window or cell wall, respectively, to a high resolution visible spectrometer with a resolution of $\pm 0.006\,nm$ over the spectral range $190-860\,nm$. The spectrometer was a Jobin Yvon Horiba 1250 M with 2400 groves/mm ion-etched holographic diffraction grating. The entrance and exit slits were set to $20\,\mu m$. The spectrometer was scanned between $655.5-657\,nm$ using a $0.01\,nm$ step size. The signal was recorded by a PMT with a stand alone high voltage power supply (950 V) and an acquisition controller. The data was obtained in a single accumulation with a 1 second integration time.

In addition, the high resolution visible spectrum of each rt-plasma was recorded over the range $400-410\,nm$ using the same methods as those

of the line broadening measurements. The emission from a control hydrogen microwave discharge plasma maintained by the methods given previously [18] was also recorded.

B. Calvet calorimeter methods for the power balance measurement of a rt-plasma formed with K^+/K^*

The power balance of a rt-plasma formed with K^+/K^* was measured calorimetrically using Calvet calorimeter as shown in Figure 2. The instrument used to measure the heat of reaction comprises a cylindrical heat flux calorimeter (International Thermal Instrument Co., Model CA-100-1). The cylindrical calorimeter walls contain a thermopile structure composed of two sets of thermoelectric junctions. One set of junctions is in thermal contact with the internal calorimeter wall, at temperature T_i, and the second set of thermal junctions is in thermal contact with the external calorimeter wall at T_e which is held constant by a forced convection oven. When heat is generated in the calorimeter cell, the calorimeter radially transfers a constant fraction of this heat into the surrounding heat sink. As heat flows a temperature gradient, $(T_i - T_e)$, is established between the two sets of thermopile junctions. This temperature gradient generates a voltage which is compared to the linear voltage versus power calibration curve to give the power of the reaction. The calorimeter was calibrated with a filament that served as a joule heater and a fixed power source at power levels representative of the power of reaction of the catalyst runs. The calibration constant of the Calvet calorimeter is not sensitive to the flow of hydrogen over the range of conditions of the tests. A chemically resistant cylindrical reactor, machined from 304 stainless steel to fit inside the calorimeter, was used to contain the reaction. To maintain an isothermal reaction system and improve baseline stability, the calorimeter was placed inside a commercial forced convection oven (Precision Scientific 625 S) capable of operating from room temperature to $616\,K$. Also, the calorimeter and reactor were enclosed within a cubic insulated box filled with aluminasilicate insulation to further dampen thermal oscillations in the oven. A more complete description of the instrument and methods are given by Bradford, Phillips, and Klanchar [46].

C. Gas Cell for Calvet Calorimeter

Since KNO_3 is volatile at a temperature much less than that at which it decomposes [47], it was used as the source of K^+/K^* catalyst at a temperature at which it was volatile. The cylindrical stainless steel filament cell and Calvet instrument for power balance studies with hydrogen and gaseous KNO_3 compared to gaseous KNO_3 alone is shown in Figure 2. The cell schematic is shown in Figure 3. The cell comprised a 20 cc stainless steel vessel. The cell was maintained at a constant isothermal temperature of 250 °C by the forced convection oven. The cell was used in the vertical position and was inserted into a thermopile. The flange was sealed with a copper gasket. The flange had a two hole Conax-Buffalo gland for the leads of a 0.25 mm diameter by 10, 20, or 30 cm length Pt (Aldrich 99.99%) filament wound in a coil that radiatively heated a 0.7 ml volume, cylindrical flat base Alumina crucible (Alfa 15 mm high X10 mm OD X 8 mm ID) which contained 250 mg of KNO_3 (Aldrich 99.999% pure). The filament served to dissociate hydrogen and to slowly vaporize the KNO_3 by heating. The filament also served as a precision resistor to calibrate the cell. The filament was powered by a constant power supply (Pennsylvania State University 0-20 W ± 1%), and the power dissipated in the filament was recorded with a watt meter (Clarke-Hess Model 259 V-A-W Meter ± 0.03 W).

The flange also had a 6.4 mm vacuum port through which a 1.6 mm OD inlet for hydrogen passed. The hydrogen gas was ultrahigh pure grade or higher (Praxair). The 1.6 mm OD inlet was connected to a 6.4 mm OD stainless steel tube which connected to a Tee, a needle valve, a pressure gauge, and then the gas supply. The elbow port of the Tee was attached to a vacuum gauge, a needle valve, a meter valve, and then a vacuum pump. The gas pressure was controlled manually by adjusting the supply through the inlet versus the amount pumped away at the outlet where the pressure was monitored in the outlet tube by the vacuum gauge. The hydrogen pressure and flow rate were adjusted to maximize the output power. The optimal pressure was about 0.2 torr maintained by an estimated flow rate of about 0.1 sccm. The data was recorded with a data acquisition system.

The cell was calibrated by measuring the steady state Calvet response to constant power into the filament over the power range 1-16 W with hydrogen at 0.2 Torr pressure without KNO_3. At a constant oven temperature of 250 °C, the experiment was repeated by allowing the Calvet voltage to reach steady state with KNO_3 alone present and constant power applied to the filament. Hydrogen was then maintained at 0.2 Torr with flow. The experiment was performed for a filament length of 10, 20, or 30 cm at a constant filament input power of 7.02, 9.82, and 15.01 W, respectively.

D. Calvet power balance measurements

Since the ambient temperature was held constant, the general form of the power balance equation for the Calvet cell in steady state is:

$$0 = P_{in} + P_{ex} - P_{loss} \tag{1}$$

where P_{in} is the input power to the filament, P_{ex} is the excess power generated from the hydrogen catalysis reaction, and P_{loss} is the thermal power loss from the cell. The Calvet voltage response to input power for hydrogen without KNO_3 was determined over the constant input power range of 1 W to 16 W. The data was recorded after the cell had reached a thermal steady state with each increase in the input power to the filament which typically occurred in about 6 hours. At this point, the power lost from the cell P_{loss} was equal to the total power P_T supplied to the cell P_{in} plus any excess power P_{ex}.

$$P_T = P_{in} + P_{ex} = P_{loss} \tag{2}$$

Since the heat transfer was dominated by conduction, the output voltage of the cell V was modeled by a linear curve

$$V = aP_T + C \tag{3}$$

where a and C are constants for the least square curve fit of the Calvet voltage response to power input for the control experiments ($P_{ex} = 0$). V was recorded as a function of input power P_{in} for hydrogen without KNO_3 catalyst as the input power was varied. The higher voltage produced with hydrogen and catalyst compared with hydrogen and no catalyst was representative of the excess power. In the case of the catalysis run, the total output power P_T was determined by solving Eq. (3) using the measured V. The excess power P_{ex} was determined from Eq. (2). The

integral of the excess power P_{ex} over time gave the excess energy E_{ex}.

E. Filament cell apparatus and procedure for power balance measurement of an Ar^{+} rt-plasma

The power balance of a rt-plasma of strontium with argon-hydrogen mixture (95/5%) was measured with the experimental setup shown in Figure 4. The power balances of argon-hydrogen-strontium rt-plasmas maintained in a one-liter cylindrical stainless steel cell fitted with a heated tungsten filament shown in Figure 5 were measured by heat loss calorimetry (determining the power balance from the temperature at steady state relative to that of a control power source) as the input power to the filament was varied. The relationship between the rate of heat loss from the cell and the cell temperature was determined from a control experiment in which both strontium catalyst and plasma were absent.

The 304-stainless steel cylindrical cell was 9.21 cm in diameter and 14.5 cm in height. The base of the cell contained a welded-in stainless steel thermocouple well (1 cm OD) which housed a thermocouple in the cell interior approximately 3 cm from the cell axis. The upper end of the cell was welded to a high vacuum 15 cm diameter conflat flange. A silver-plated copper gasket was used to seal the cell flange to a mating flange. The two flanges were clamped together with 10 circumferential bolts. The mating flange contained two penetrations comprising a stainless steel thermocouple well (1 cm OD), which also housed a thermocouple in the cell interior approximately 3.5 cm from the cell axis, and a centered high voltage feedthrough. The body of the cell included two radial penetrations. One was a 9.5 mm OD tube for gas fill and evacuation, the other was a tube which housed a 1.5 cm diameter UV-grade sapphire viewport. The cell interior was fitted with a 27 mm OD grooved Alumina tube which was 60 mm in length. The tube was tightly wrapped with approximately 330 cm of 0.25 mm tungsten wire. The tube was suspended on the cell axis by connecting the ends of the tungsten filament to the central electrode and the cell body (ground) as shown in Figure 5. AC power at 60 Hz was supplied to the filament through a variac. True rms voltage and current, and also power

dissipation in the filament were monitored by a digital volt-amp-watt meter (Clarke-Hess Model 259 V-A-W Meter) shown in Figure 4. Gas pressure in the cell was monitored with a 0-10 Torr MKS Baratron absolute pressure gauge.

Approximately 1.2 g of strontium metal (Alfa Aesar 99.95%) was placed on the base of the cell under one atmosphere of dry argon in a glovebox. After sealing the cell it was heated in a temperature-controlled kiln to 465°C while evacuating the system. At this condition the strontium vapor pressure was approximately 1 mTorr. After reaching thermal equilibrium, the cell was pressurized with 190 mTorr of argon and then an additional 10 mTorr of hydrogen to yield a argon-hydrogen mixture (95/5%) at 200 mTorr. Hydrogen was periodically added during the course of the experiment in order to maintain 200 mTorr pressure. It was observed that a substantial amount of hydrogen was absorbed during addition which was attributed to formation of strontium hydride. Ultrahigh purity grade argon and hydrogen were used. Approximately 50 V was applied to the filament corresponding to about 100 W. Plasma formation resulted after several minutes of heating the cell with the filament. Strong strontium and argon plasma line emission were observed in the visible and near-infrared with a visible spectrometer (Ocean Optics S2000). Electric power input to the cell was varied in the range 110-245 W. At each power setting, 2.5-3 hours was allowed for the cell to reach thermal equilibrium. The cell temperature was then computed by averaging the temperatures of the two thermocouples. In the control experiment, this procedure was repeated with the same cell except that both strontium and the resulting rt-plasma were absent.

G. Filament cell power balance measurements

Heat loss from the cell was primarily by radiation. Because the temperature of the kiln was fixed, the rate of heat loss from the cell, $P_T = P_{loss}$, was a function of the cell temperature:

$$P_T = f(T) \tag{4}$$

This relationship was determined from the argon-hydrogen control experiments in which $P = P_{in}$ was the electric power input. In the argon-hydrogen-strontium rt-plasma experiments, the rate of heat loss from

the cell exceeded the electric power input by the excess power P_{ex}

$$P_T = P_{in} + P_{ex} = f(T) \quad (5)$$

The excess power was then

$$P_{ex} = P_T - P_{in} = f(T) - P_{in} \quad (6)$$

Using the measured cell temperature and the input power, the excess power of each argon-hydrogen-strontium rt-plasma was computed from Eq. (6).

III. RESULTS

A. Balmer line broadening and high resolution visible spectroscopy recorded on rt-plasmas

The results of the 656.2 nm Balmer α line width measured with a high resolution ($\pm 0.006\ nm$) visible spectrometer on light emitted from rt-plasmas of hydrogen with K_2CO_3, $RbNO_3$, Cs_2CO_3, and $SrCO_3$, and $SrCO_3$ with an argon-hydrogen mixture (97/3%) are shown in Figures 6-10, respectively. The spectrum of the KNO_3 cell was the same as that of the K_2CO_3 cell except that the intensity was higher. To illustrate the method of displaying each line broadening result as an unsmoothed curve, the corresponding raw data points are also shown in Figures 9 and 10 that further show the scatter in the data. The Balmer α line width and energetic hydrogen atom densities and energies given in Table 1 were calculated using the method of Videnocic et al. [8]. Significant line broadening of 17, 9, 11, 14, *and* 24 *eV* and an atom density of $4\ X\ 10^{11}$, $6\ X\ 10^{11}$, $4\ X\ 10^{11}$, $8\ X\ 10^{11}$, *and* $4\ X\ 10^{11}$ *atoms/cm*^{3} were observed from a rt-plasma of hydrogen formed with K^+/K^+, Rb^+, cesium, strontium, and strontium with Ar^+ catalysts, respectively. A glow discharge of hydrogen maintained at the same total pressure showed no excessive broadening corresponding to an average hydrogen atom temperature of $\approx 3\ eV$. The superposition of the 656 nm Balmer α line width recorded with a high resolution ($\pm 0.006\ nm$) visible spectrometer on a hydrogen-strontium rt-plasma and a hydrogen-strontium rt-plasma intensified by argon ion catalyst is shown in Figure 11. By comparison to the strontium rt-plasma, significant broadening attributable to argon ion was observed corresponding to an average hydrogen atom temperature of 24 *eV* versus

14 eV. The atom density was also very high in the argon rt-plasma given that the hydrogen concentration was 30 times less than that of the strontium-pure-hydrogen rt-plasma.

The high resolution visible spectra in the region of 407 nm from the hydrogen rt-plasma formed using K_2CO_3, $RbNO_3$, Cs_2CO_3, and strontium metal with argon are shown in Figures 12-15, respectively. In each case, a peak was observed at 407 nm which could not be assigned to hydrogen, alkali or alkaline earth atom or ion. The know peaks of these atoms and ions in the region of 407 nm were separated as indicated in the figures. The spectrum of the KNO_3 cell was the same as that of the K_2CO_3 cell.

The 407.0 nm peak was not observed in an intense hydrogen microwave discharge plasma as shown in Figure 16. O II lines at 406.9623, 406.9881, and 407.1238 nm were eliminated due to the absence of OI lines at 394.729, 394.748, 394.758, 395.460, and 405.477 nm. CIII lines at 407.026 and 406.8916 nm were eliminated due to the absence of CI lines which were outside of the region of 407 nm or CII lines at 391.896 and 392.068 nm. The observation of the 407.0 peak with KNO_3, $RbNO_3$, and with strontium metal and argon also eliminated carbon as the source of the novel peak. Furthermore, the presence of the OII or CIII lines would be extraordinary since the ionization energy required for OII is above the first ionization energy of 13.62 eV, and the energies required for CIII are above the sum of the first and second ionization energies of 11.26 eV and 24.38 eV, respectively [48].

The emission intensity and the Balmer α line broadening of the hydrogen rt-plasma formed using strontium metal or $SrCO_3$ increased significantly with the introduction of argon gas only when Ar^+ emission was observed as shown in Figure 11. In both cases, the 407 nm peak of the argon-hydrogen-strontium rt-plasma was not observed with hydrogen alone—the presence of Ar^+ was required. The 407 nm peak shown in Figure 15 was formed using argon with strontium metal with no oxygen or carbon present which further eliminated oxygen and carbon lines as possible sources.

B. Power balance of a K^+/K^+ rt-plasma

The Calvet voltage as a function of the power applied to the

filament heater at 0.2 Torr hydrogen pressure was plotted for the input power range of 0.5 W to 16 W as shown in Figure 17. The least squares fit of the V response to unit input power calculated from the control (Eq. (3)) was determined to be

$$V = -0.061 + 0.233 \times P_T \tag{7}$$

A constant filament input power of 7.02, 9.82, and 15.01 W was maintained for a filament length of 10, 20, or 30 cm, respectively. The Calvet voltage was allowed to reach steady state with KNO_3 alone. The Calvet voltage significantly increased upon the addition of hydrogen, and the output signal was permitted to reach a second steady state as shown in Figure 18 for the case of 9.82 W input to a 20 cm long filament with a typical voltage and current of 4.16 V and 2.36 A, respectively. The excess power in each case was determined from Eq. (7) and Eq. (2). The results are shown in Table 2.

The sources of error were the error in the calibration curve (± 0.05 W) and the power measurement of the watt meter (± 0.03 W) in the power range of 0-16 W which was independent of the errors of the voltage ($\pm 0.025\ V$) and current ($\pm 1\ mA$) measurements due to any power factor. The propagated error of the calibration and power measurements was ± 0.06 W.

C. Power balance of an Ar^+ rt-plasma

Power input to the cell is plotted versus the cell temperature for the argon-hydrogen-strontium rt-plasma and also for the argon-hydrogen control in Figure 19. The relation between cell temperature and the rate of heat loss from the cell, found from the argon-hydrogen control data, is of the form

$$P_T = f(T) = A\left(T^4 - T_0^4\right) \tag{8}$$

where $A = 2.74\ X\ 10^{-9}\ W/K^4$ and T_0 = 465°C = 738.2 K is the kiln temperature. Deviations of the control data from this expression are less than 2 W. Using Eq. (8) in Eq. (6) yields the excess power generated in the argon-hydrogen-strontium rt-plasma for each power input condition. Power input and excess power are tabulated in Table 3. The excess power ranged from 13.3 W at 110 W input to 26.0 W at 245 W input. The average excess power over the range was about 20 W. This

corresponded to an excess power density of approximately 20 mW/cc in the one-liter cell.

The error in the temperature measurement over the range of 70 °C was $\pm 0.5\,°C$ for the type K thermocouples. However, the excess power was measured as the difference in filament power to the control to achieve the same temperature as the argon-hydrogen-strontium rt-plasma. Thus, the sources of error were the error in the calibration curve $\pm 2\,W$ and the power measurement of the watt meter ($\pm 1\,W$) in the power range of 100-300 W which was independent of the errors of the voltage ($\pm 0.25\,V$) and current ($\pm 10\,mA$) measurements due to any power factor. The propagated error of the calibration and power measurements was $\pm 2.2\,W$.

IV. DISCUSSION

Line broadening of the hydrogen Balmer lines provides a sensitive measure of the number and energy of excited hydrogen atoms in a plasma. To further characterize the plasma parameters of rt-plasmas, the width of the 656.2 nm Balmer α line was recorded on light emitted from rt-plasmas formed from hydrogen with a gaseous atom or ion which ionizes at integer multiples of the potential energy of atomic hydrogen. The energetic hydrogen atom density and energies were determined from the broadening, and it was found that significant line broadening of 17, 9, 11, 14, *and* 24 eV and an atom density of $4\,X\,10^{11}$, $6\,X\,10^{11}$, $4\,X\,10^{11}$, $8\,X\,10^{11}$, *and* $4\,X\,10^{11}$ $atoms/cm^3$ were observed from a rt-plasma of hydrogen formed with K^+/K^+, Rb^+, cesium, strontium, and strontium with Ar^+ catalysts, respectively. Whereas, a glow discharge of hydrogen maintained at the same total pressure with an electric field strength that was at least two order of magnitude greater than the 1 V/cm field of the filament cell showed no excessive broadening corresponding to an average hydrogen atom temperature of $\approx 3\,eV$.

In the characterization of the plasmas of Grimm-type discharges with a hollow anode, M. Kuraica and N. Konjevic [7] and Videnocic et al. [8] analyzed the broadening data in terms of Stark and Doppler effects wherein acceleration of charges such as H^+, H_2^+, and H_3^+ in the high fields (e. g. over $10\,kV/cm$) which were present in the cathode fall region was

used to explain the Doppler component. In our experiments, the results could not be explained by Stark or thermal broadening or electric field acceleration of charged species since the measured field of the incandescent heater was extremely weak, 1 V/cm, corresponding to a broadening much less than $1\,eV$. Rather the source of the excessive line broadening is consistent with that of EUV emission, an energetic reaction caused by a resonance energy transfer between hydrogen atoms and K^+/K^+, Rb^+, cesium, strontium, or Ar^+ catalysts.

Rt-plasmas formed with hydrogen-potassium mixtures have been reported previously [34-35] wherein the plasma decayed with a two second half-life when the electric field was set to zero. This was the thermal decay time of the filament which dissociated molecular hydrogen to atomic hydrogen. This experiment showed that hydrogen line emission was occurring even though the voltage between the heater wires was set to and measured to be zero and indicated that the emission was due to a reaction of potassium atoms with atomic hydrogen. Potassium atoms ionize at an integer multiple of the potential energy of atomic hydrogen, $m \cdot 27.2\,eV$. The enthalpy of ionization of K to K^{3+} has a net enthalpy of reaction of $81.7426\,eV$, which is equivalent to $m = 3$.

A rt-plasma of hydrogen and certain alkali ions formed at low temperatures (e.g. $\approx 10^3\,K$) as recorded via EUV spectroscopy and the hydrogen Balmer and alkali line emissions in the visible range [35]. The observed plasma formed at low temperatures (e.g. $\approx 10^3\,K$) from atomic hydrogen generated at a tungsten filament that heated a titanium dissociator and one of potassium, rubidium, cesium, and their carbonates and nitrates. These atoms and ions ionize to provide a net enthalpy of reaction of an integer multiple of the potential energy of atomic hydrogen ($m \cdot 27.2\,eV$, $m = \text{integer}$) to within 0.17 eV and comprise only a single ionization in the case of a potassium or rubidium ion. Whereas, the chemically similar atoms of sodium and sodium and lithium carbonates and nitrates which do not ionize with these constraints caused no emission. To test the electric dependence of the emission, the weak electric field of about 1 V/cm was set and measured to be zero in $< 0.5\,X\,10^{-6}$ sec. An afterglow duration of about one to two seconds was recorded in the case of potassium, rubidium, cesium, K_2CO_3, $RbNO_3$, and $CsNO_3$. Hydrogen line or alkali line emission was occurring even though

the voltage between the heater wires was set to and measured to be zero. These atoms and ions ionize to provide a net enthalpy of reaction of an integer multiple of the potential energy of atomic hydrogen to within less than the thermal energies at $\approx 10^3\,K$ and comprise only a single ionization in the case of a potassium or rubidium ion. Since the thermal decay time of the filament for dissociation of molecular hydrogen to atomic hydrogen was similar to the rt-plasma afterglow duration, the emission was determined to be due to a reaction of atomic hydrogen with each of the atoms or ions that did not require the presence of an electric field to be functional.

Each of K^+/K^+, Rb^+, Cs, and Ar^+ as the catalyst are predicted to catalyze hydrogen to form $H\left[\frac{a_H}{2}\right]$ which reacts with an electron to form $H^-(1/2)$. The predicted $H^-(1/2)$ hydride ion of hydrogen catalysis by these catalysts was observed spectroscopically at $407\,nm$ corresponding to its predicted binding energy of $3.05\,eV$. The hydride reaction product formed over time.

The release of energy from hydrogen as evidenced by the EUV emission must result in a lower-energy state of hydrogen. The present study identified the formation of a novel hydride ion, $H^-(1/2)$. The formation of novel compounds based on novel hydride ions would be substantial evidence supporting catalysis of hydrogen as the mechanism of the observed EUV emission and further support the present spectroscopic identification of $H^-(1/2)$. Compounds containing novel hydride ions have been isolated as products of the reaction of atomic hydrogen with atoms and ions identified as catalysts in the present study and previously reported EUV studies [18-25, 31-42]. The novel hydride compounds were identified analytically by techniques such as time of flight secondary ion mass spectroscopy, X-ray photoelectron spectroscopy, and ^1H nuclear magnetic resonance spectroscopy. For example, the time of flight secondary ion mass spectroscopy showed a large hydride peak in the negative spectrum. The X-ray photoelectron spectrum showed large metal core level shifts due to binding with the hydride as well as novel hydride peaks. The ^1H nuclear magnetic resonance spectrum showed significantly upfield shifted peaks which corresponded to and identified novel hydride ions.

Balmer α line broadening and the predicted $407\,nm$ peak corresponding to the hydride ion product $H^-(1/2)$ was observed in the case of potassium ions as the catalyst. Thus, the power balance of a rt-plasma formed with KNO_3 which is volatile under the measurement conditions of $250\,°C$ was determined using Calvet calorimetry. The steady state Calvet voltage significantly increased upon the addition of atomic hydrogen to vaporized KNO_3. With constant power per unit length to the filament to maintain a constant filament temperature, the power was observed to be linear in filament length, and therefore filament area. This result is consistent with the dissociation of hydrogen as a rate limiting mechanism. Given a flow rate of 0.1 sccm and an excess power of 2.07 W, energy balances of over $-28{,}000\,kJ/mole\,H_2$ ($145\,eV/H\,atom$) were measured. The reduction of KNO_3 to water, potassium metal, and NH_3 calculated from the heats of formation only releases $-14.2\,kcal/mole\,H_2$ ($0.3\,eV/H\,atom$) which can not account for the observed heat.

$$9/2H_2 + KNO_3 \rightarrow K + 3H_2O + NH_3 \qquad \Delta H = -14.2\,kcal/mole\,H_2 \tag{9}$$

The most energetic reaction possible was the reaction of hydrogen to form water which releases $-241.8\,kJ/mole\,H_2$ ($1.48\,eV/H\,atom$) which is about 100 times less than that observed. The results indicate that once a hydrino atom is formed by a catalyst, further catalytic transitions: $n=\frac{1}{2}\rightarrow\frac{1}{3}$, $\frac{1}{3}\rightarrow\frac{1}{4}$, $\frac{1}{4}\rightarrow\frac{1}{5}$, and so on occur to a substantial extent. This is consistent with the previously given theory [12, 18, 20, 27], the reported series of lower-energy hydrogen lines with energies of $q\cdot 13.6\,eV$ where $q=1,2,3,4,6,7,8,9,\,or\,11$ [18-19, 27], and previous studies which show very large energy balances [26-27, 29-30].

Similarly, the emission intensity of the plasma generated by atomic strontium increased significantly with the introduction of argon gas only when Ar^+ emission was observed. And, an increase in the Balmer α line broadening and the predicted $407\,nm$ peak corresponding to the hydride ion product $H^-(1/2)$ was observed with Ar^+ present as the catalyst. Thus, the power balance of a rt-plasma formed with Ar^+ as the catalyst was measured by heat loss calorimetry. The steady state temperature of a rt-plasma formed with strontium and increased by Ar^+ was significantly higher than heated argon which did not form a rt-plasma. A maximum excess power of 26 W was observed. The enthalpy of formation ΔH_p of

strontium hydride is $-47.59\ kcal/mole$ ($1.0\ eV/H\ atom$) [49]. Thus, the energy for hydriding all of the 1.2 g (13 mmoles) of strontium would be 0.65 kcal compared to the energy released over the minimum three hours to steady state of 280 kcal.

IV. CONCLUSION

Each of the ionization of Rb^+, cesium, strontium and Ar^+, and an electron transfer between two K^+ ions provide a reaction with a net enthalpy of an integer multiple of the potential energy of atomic hydrogen. The presence of each of the corresponding reactants formed the low applied temperature, extremely low voltage plasma called a resonance transfer or rt-plasma. For further characterization, the width of the 656.2 nm Balmer α line was recorded on light emitted from rt-plasmas. Significant line broadening of 17, 9, 11, 14, *and* 24 eV was observed from a rt-plasma of hydrogen formed with K^+/K^+, Rb^+, Cs, and Ar^+ catalysts, respectively. These results could not be explained by Stark or thermal broadening or electric field acceleration of charged species since the measured field of the incandescent heater was extremely weak, 1 V/cm, corresponding to a broadening much less than $1\ eV$. Rather, the source of the excessive line broadening is consistent with that of EUV emission, an energetic reaction caused by a resonance energy transfer between hydrogen atoms and the catalyst. Since line broadening is a measure of temperature, the excess power of about 20 mW/cc was measured calorimetrically on K^+/K^+ and Ar^+ catalyzed rt-plasmas corresponding to an energy balance of about 100 times that of the combustion of the hydrogen. The product hydride ion with each of K^+/K^+, Rb^+, Cs, and Ar^+ as the catalyst was predicted to have a binding energy of $3.05\ eV$ and was observed by high resolution visible spectroscopy at the corresponding $407\ nm$.

Since the net enthalpy released may be at least one hundred times that of combustion, the catalysis of atomic hydrogen represents a new source of energy with H_2O as the source of hydrogen fuel. Moreover, rather than air pollutants or radioactive waste, novel hydride compounds with potential commercial applications are the products [36-42]. Since the power is in the form of a plasma, direct high-efficiency, low cost

energy conversion may be possible, thus, avoiding a heat engine such as a turbine [43-45] or a reformer-fuel cell system. Significantly lower capital costs and lower commercial operating costs than that of any known competing energy source are anticipated.

ACKNOWLEDGMENT

Special thanks to Alex Echezuria for preparing filament cells for plasma experiments.

REFERENCES

1. P. W. J. M. Boumans, Spectrochim. Acta Part B, 46 (1991) 711.
2. J. A. C. Broekaert, Appl. Spectrosc., 49, (1995) 12A.
3. P. W. J. M. Boumans, J. A. C. Broekaert, and R. K. Marcus, Eds., Spectrochim. Acta Part B, 46 (1991) 457.
4. M. Dogan, K. Laqua, and H. Massmann, "Spektrochemische Analysen mit einer Glimmentladungslampe als Lichtquelle—I," Spectrochim. Acta, Volume 26B, (1971) 631–649.
5. M. Dogan, K. Laqua, and H. Massmann, "Spektrochemische Analysen mit einer Glimmentladungslampe als Lichtquelle—II, "Spectrochim. Acta, Volume 27B, (1972) 65–88.
6. J. A. C. Broekaert, J. Anal. At. Spectrom., 2 (1987) 537.
7. M. Kuraica, N. Konjevic, "Line shapes of atomic hydrogen in a plane-cathode abnormal glow discharge", Physical Review A, Volume 46, No. 7, October (1992), pp. 4429-4432.
8. I. R. Videnocic, N. Konjevic, M. M. Kuraica, "Spectroscopic investigations of a cathode fall region of the Grimm-type glow discharge", Spectrochimica Acta, Part B, Vol. 51, (1996), pp. 1707-1731.
9. P. Kurunczi, H. Shah, and K. Becker, "Hydrogen Lyman-α and Lyman-β emissions from high-pressure microhollow cathode discharges in $Ne-H_2$ mixtures", J. Phys. B: At. Mol. Opt. Phys., Vol. 32, (1999), L651-L658.
10. M. Parker and R. K. Marcus, Appl. Spectrosc., 48, (1994) 623.
11. J. A. R. Sampson, *Techniques of Vacuum Ultraviolet Spectroscopy*, Pied

Publications, (1980), pp. 94-179.
12. R. Mills, *The Grand Unified Theory of Classical Quantum Mechanics*, January 2000 Edition, BlackLight Power, Inc., Cranbury, New Jersey, Distributed by Amazon.com; September 2001 Edition posted at www.blacklightpower.com.
13. R. Mills, "The Grand Unified Theory of Classical Quantum Mechanics", Global Foundation, Inc. Orbis Scientiae entitled *The Role of Attractive and Repulsive Gravitational Forces in Cosmic Acceleration of Particles The Origin of the Cosmic Gamma Ray Bursts*, (29th Conference on High Energy Physics and Cosmology Since 1964) Dr. Behram N. Kursunoglu, Chairman, December 14-17, 2000, Lago Mar Resort, Fort Lauderdale, FL.
14. R. Mills, "The Grand Unified Theory of Classical Quantum Mechanics", Global Foundation, Inc. Orbis Scientiae entitled *The Role of Attractive and Repulsive Gravitational Forces in Cosmic Acceleration of Particles The Origin of the Cosmic Gamma Ray Bursts*, (29th Conference on High Energy Physics and Cosmology Since 1964) Dr. Behram N. Kursunoglu, Chairman, December 14-17, 2000, Lago Mar Resort, Fort Lauderdale, FL, Kluwer Academic/Plenum Publishers, New York, pp. 243-258.
15. R. Mills, "The Grand Unified Theory of Classical Quantum Mechanics", Int. J. of Hydrogen Energy, in press.
16. R. Mills, "The Hydrogen Atom Revisited", Int. J. of Hydrogen Energy, Vol. 25, Issue 12, December, (2000), pp. 1171-1183.
17. R. Mills, The Nature of Free Electrons in Superfluid Helium—a Test of Quantum Mechanics and a Basis to Review its Foundations and Make a Comparison to Classical Theory, Int. J. Hydrogen Energy, Vol. 26, No. 10, (2001), pp. 1059-1096.
18. R. Mills, P. Ray, "Spectral Emission of Fractional Quantum Energy Levels of Atomic Hydrogen from a Helium-Hydrogen Plasma and the Implications for Dark Matter", Int. J. Hydrogen Energy, in press.
19. R. L. Mills, P. Ray, B. Dhandapani, J. He, "Spectroscopic Identification of Fractional Rydberg States of Atomic Hydrogen" J. Phys. Chem., submitted.
20. R. Mills, P. Ray, "Vibrational Spectral Emission of Fractional-Principal-Quantum-Energy-Level Hydrogen Molecular Ion", Int. J. Hydrogen Energy, in press.

21. R. L. Mills, P. Ray, "Spectroscopic Identification of a Novel Catalytic Reaction of Rubidium Ion with Atomic Hydrogen and the Hydride Ion Product", Int. J. Hydrogen Energy, submitted.
22. R. Mills, P. Ray, Spectroscopic Identification of a Novel Catalytic Reaction of Potassium and Atomic Hydrogen and the Hydride Ion Product, Int. J. Hydrogen Energy, in press.
23. R. Mills, "Spectroscopic Identification of a Novel Catalytic Reaction of Atomic Hydrogen and the Hydride Ion Product", Int. J. Hydrogen Energy, Vol. 26, No. 10, (2001), pp. 1041-1058.
24. R. Mills and M. Nansteel, "Argon-Hydrogen-Strontium Plasma Light Source", IEEE Transactions on Plasma Science, submitted.
25. R. Mills, M. Nansteel, and Y. Lu, "Excessively Bright Hydrogen-Strontium Plasma Light Source Due to Energy Resonance of Strontium with Hydrogen", European Journal of Physics D, submitted.
26. R. Mills, J. Dong, W. Good, P. Ray, J. He, B. Dhandapani, Measurement of Energy Balances of Noble Gas-Hydrogen Discharge Plasmas Using Calvet Calorimetry, Int. J. Hydrogen Energy, submitted.
27. Randell L. Mills, P. Ray, B. Dhandapani, M. Nansteel, X. Chen, J. He, "New Power Source from Fractional Quantum Energy Levels of Atomic Hydrogen that Surpasses Internal Combustion", Spectrochimica Acta, submitted.
28. R. L. Mills, P. Ray, B. Dhandapani, J. He, "Comparison of Excessive Balmer α Line Broadening of Glow Discharge and Microwave Hydrogen Plasmas with Certain Catalysts" J. Phys. Chem., submitted.
29. R. L. Mills, A. Voigt, P. Ray, M. Nansteel, B. Dhandapani, "Measurement of Hydrogen Balmer Line Broadening and Thermal Power Balances of Noble Gas-Hydrogen Discharge Plasmas", Int. J. Hydrogen Energy, in press.
30. R. Mills, N. Greenig, S. Hicks, "Optically Measured Power Balances of Anomalous Discharges of Mixtures of Argon, Hydrogen, and Potassium, Rubidium, Cesium, or Strontium Vapor", Int. J. Hydrogen Energy, in press.
31. R. Mills, M. Nansteel, and Y. Lu, "Observation of Extreme Ultraviolet Hydrogen Emission from Incandescently Heated Hydrogen Gas with Strontium that Produced an Anomalous Optically Measured Power Balance", Int. J. Hydrogen Energy, Vol. 26, No. 4, (2001), pp. 309-326.

32. R. Mills, J. Dong, Y. Lu, "Observation of Extreme Ultraviolet Hydrogen Emission from Incandescently Heated Hydrogen Gas with Certain Catalysts", Int. J. Hydrogen Energy, Vol. 25, (2000), pp. 919-943.
33. R. Mills, "Observation of Extreme Ultraviolet Emission from Hydrogen-KI Plasmas Produced by a Hollow Cathode Discharge", Int. J. Hydrogen Energy, Vol. 26, No. 6, (2001), pp. 579-592.
34. R. Mills, "Temporal Behavior of Light-Emission in the Visible Spectral Range from a Ti-K2CO3-H-Cell", Int. J. Hydrogen Energy, Vol. 26, No. 4, (2001), pp. 327-332.
35. R. Mills, T. Onuma, and Y. Lu, "Formation of a Hydrogen Plasma from an Incandescently Heated Hydrogen-Catalyst Gas Mixture with an Anomalous Afterglow Duration", Int. J. Hydrogen Energy, Vol. 26, No. 7, July, (2001), pp. 749-762.
36. R. Mills, B. Dhandapani, M. Nansteel, J. He, A. Voigt, "Identification of Compounds Containing Novel Hydride Ions by Nuclear Magnetic Resonance Spectroscopy", Int. J. Hydrogen Energy, Vol. 26, No. 9, Sept. (2001), pp. 965-979.
37. R. Mills, B. Dhandapani, N. Greenig, J. He, "Synthesis and Characterization of Potassium Iodo Hydride", Int. J. of Hydrogen Energy, Vol. 25, Issue 12, December, (2000), pp. 1185-1203.
38. R. Mills, "Novel Inorganic Hydride", Int. J. of Hydrogen Energy, Vol. 25, (2000), pp. 669-683.
39. R. Mills, "Novel Hydrogen Compounds from a Potassium Carbonate Electrolytic Cell", Fusion Technology, Vol. 37, No. 2, March, (2000), pp. 157-182.
40. R. Mills, B. Dhandapani, M. Nansteel, J. He, T. Shannon, A. Echezuria, "Synthesis and Characterization of Novel Hydride Compounds", Int. J. of Hydrogen Energy, Vol. 26, No. 4, (2001), pp. 339-367.
41. R. Mills, "Highly Stable Novel Inorganic Hydrides", Journal of New Materials for Electrochemical Systems, in press.
42. R. Mills, W. Good, A. Voigt, Jinquan Dong, "Minimum Heat of Formation of Potassium Iodo Hydride", Int. J. Hydrogen Energy, Vol. 26, No. 11, Oct., (2001), pp. 1199-1208.
43. R. Mills, "BlackLight Power Technology-A New Clean Hydrogen Energy Source with the Potential for Direct Conversion to Electricity", Proceedings of the National Hydrogen Association, 12 th Annual U.S.

Hydrogen Meeting and Exposition, *Hydrogen: The Common Thread*, The Washington Hilton and Towers, Washington DC, (March 6-8, 2001), pp. 671-697.

44. R. Mills, "BlackLight Power Technology-A New Clean Energy Source with the Potential for Direct Conversion to Electricity", Global Foundation International Conference on "Global Warming and Energy Policy", Dr. Behram N. Kursunoglu, Chairman, Fort Lauderdale, FL, November 26-28, 2000, Kluwer Academic/Plenum Publishers, New York, pp. 1059-1096.
45. R. Mayo, R. Mills, M. Nansteel, "On the Potential of Direct and MHD Conversion of Power from a Novel Plasma Source to Electricity for Microdistributed Power Applications", IEEE Transactions on Plasma Science, submitted.
46. M. C. Bradford, J. Phillips, J. Klanchar, Rev. Sci. Instrum., 66, (1), January, (1995), pp. 171-175.
47. C. J. Hardy, B. O. Field, J. Chem. Soc., (1963), pp. 5130-5134.
48. David R. Linde, *CRC Handbook of Chemistry and Physics*, 79 th Edition, CRC Press, Boca Raton, Florida, (1998-9), p. 10-175 to p. 10-177.
49. W. M. Muller, J. P. Blackledge, G. G. Libowitz, *Metal Hydrides*, Academic Press, New York, (1968), p 201.

Table 1. Energetic hydrogen atom densities and energies for rt-plasmas determined from the 656.2 nm Balmer α line width.

Plasma Gas	Hydrogen Atom Density[a] (10^{11} $atoms/cm^3$)	Hydrogen Atom Energy[b] (eV)
H_2	2	2-3[c]
K/H_2	4	15-18
Rb^+/H_2	6	8-10
Cs/H_2	4	10-12
Sr/H_2	8	13-15
$Sr/Ar^+/H_2$	4	22-26

[a] Approximate Calculated [8].

[b] Calculated [8].

[c] Measured on glow discharge according to method ref. 29.

Table 2. Input and excess power for a rt-plasma formed with K^+/K^+ catalyst.

Filamnet Length (cm)	Input Power (W)	Total Power (W)[a]	Excess Power (± 0.06 W)[b]
10	7.02	7.64	0.62
20	9.82	10.63	0.81
30	15.01	17.08	2.07

[a] Eq. (7)
[b] Eq. (2)

Table 3. Input and excess power for argon-hydrogen-strontium rt-plasma.

Voltage (V)	Current (A)	Input Power (W)	Cell Temp. (K)	Total Power (W)[a]	Excess Power (± 2.2 W)[b]
40.4	2.73	110	764.7	123.3	13.3
41.7	3.04	125	768.2	140.6	15.6
43.0	3.46	140	772.1	160.1	20.1
43.4	3.57	155	775.3	176.3	21.3
44.4	3.85	170	778.6	193.3	23.3
45.7	4.27	185	780.7	204.2	19.2
46.2	4.48	200	783.7	219.9	19.9
46.8	4.70	215	786.5	234.8	19.8
47.7	4.83	230	789.3	249.8	19.8
48.4	5.17	245	793.2	271.0	26.0

[a] Eq. (8)
[b] Eq. (6)

Figure Captions

Figure 1. The experimental set up comprising a filament gas cell light source and an EUV spectrometer which was differentially pumped.

Figure 2. The Calvet instrument for power balance studies with hydrogen and gaseous KNO_3 compared hydrogen alone.

Figure 3. Schematic of the gas cell and the cross sectional view of the Calvet calorimeter used to measure the power balance of a rt-plasma formed with K^+/K^+ catalyst. 1—1.6 mm OD stainless steel tube (to hydrogen supply), 2—stainless steel tee union, 3—6.4 mm OD stainless steel tube (to vacuum manifold), 4—cell lid, 5—filament leads, 6—Conax-Buffalo gland, 7—0.1 mm OD Pt filament, 8—copper ring gasket, 9—cell body, 10—Calvet calorimeter, 11—thermopile signal output, 12—thermal shunt, 13—thermopile, 14—insulated calorimeter base, 15—Alumina crucible KNO_3 reservoir.

Figure 4. The experimental setup for generating a argon-hydrogen-strontium rt-plasma and for measuring the power balance.

Figure 5. The one-liter cylindrical stainless steel cell fitted with a heated tungsten filament used to measure the power balances of argon-hydrogen-strontium rt-plasmas as a function of input power to the filament.

Figure 6. The 656 nm Balmer α line width recorded with a high resolution ($\pm 0.006\ nm$) visible spectrometer on a rt-plasma formed with K^+/K^+ catalyst. Significant broadening was observed corresponding to an average hydrogen atom temperature of $17\ eV$.

Figure 7. The 656 nm Balmer α line width recorded with a high resolution ($\pm 0.006\ nm$) visible spectrometer on a rt-plasma formed with Rb^+ catalyst. Significant broadening was observed corresponding to an average hydrogen atom temperature of $9\ eV$.

Figure 8. The 656 nm Balmer α line width recorded with a high resolution ($\pm 0.006\ nm$) visible spectrometer on a cesium-hydrogen rt-plasma. Significant broadening was observed corresponding to an average hydrogen atom temperature of $11\ eV$.

Figure 9. The 656 nm Balmer α line width recorded with a high resolution ($\pm 0.006\ nm$) visible spectrometer on a hydrogen-strontium rt-plasma. Significant broadening was observed corresponding to an

average hydrogen atom temperature of $14\,eV$.

Figure 10. The 656 nm Balmer α line width recorded with a high resolution ($\pm 0.006\,nm$) visible spectrometer on a hydrogen-strontium rt-plasma intensified by argon ion catalyst. Significant broadening was observed corresponding to an average hydrogen atom temperature of $24\,eV$.

Figure 11. The superposition of the 656 nm Balmer α line width recorded with a high resolution ($\pm 0.006\,nm$) visible spectrometer on a hydrogen-strontium rt-plasma and a hydrogen-strontium rt-plasma intensified by argon ion catalyst. By comparison to the strontium rt-plasma, significant broadening attributable to argon ion was observed corresponding to an average hydrogen atom temperature of $24\,eV$ versus $14\,eV$.

Figure 12. The high resolution visible spectrum in the region of $407\,nm$ recorded on the emission of a rt-plasma formed with K^+/K^+ catalyst. The novel $407\,nm$ peak which could not be assigned to a known peak was assigned to $H^-(1/2)$.

Figure 13. The high resolution visible spectrum in the region of $407\,nm$ recorded on the emission of a rt-plasma formed with Rb^+ catalyst. The novel $407\,nm$ peak which could not be assigned to a known peak was assigned to $H^-(1/2)$.

Figure 14. The high resolution visible spectrum in the region of $407\,nm$ recorded on the emission of a cesium-hydrogen rt-plasma. The novel $407\,nm$ peak which could not be assigned to a known peak was assigned to $H^-(1/2)$.

Figure 15. The high resolution visible spectrum in the region of $407\,nm$ recorded on the emission of a argon-hydrogen-strontium rt-plasma. The novel $407\,nm$ peak which could not be assigned to a known peak was assigned to $H^-(1/2)$.

Figure 16. The high resolution visible spectrum in the region of $407\,nm$ recorded on the emission of a hydrogen microwave discharge plasma. The 407.0 nm peak was not observed.

Figure 17. The Calvet voltage as a function of the power applied to the 20 cm long filament with hydrogen alone at 0.2 Torr total pressure plotted for the input power range of 1 W to 16 W.

Figure 18. With 9.82 W input to the 20 cm filament, the Calvet cell

was allowed to reach a steady Calvet voltage with KNO_3 alone. The Calvet voltage significantly increased upon the addition of hydrogen, and the output signal showed 0.81 W of excess power at the second steady state.

Figure 19. Plot of power input to the cell versus the cell temperature for the argon-hydrogen-strontium plasma and also for the argon-hydrogen control.

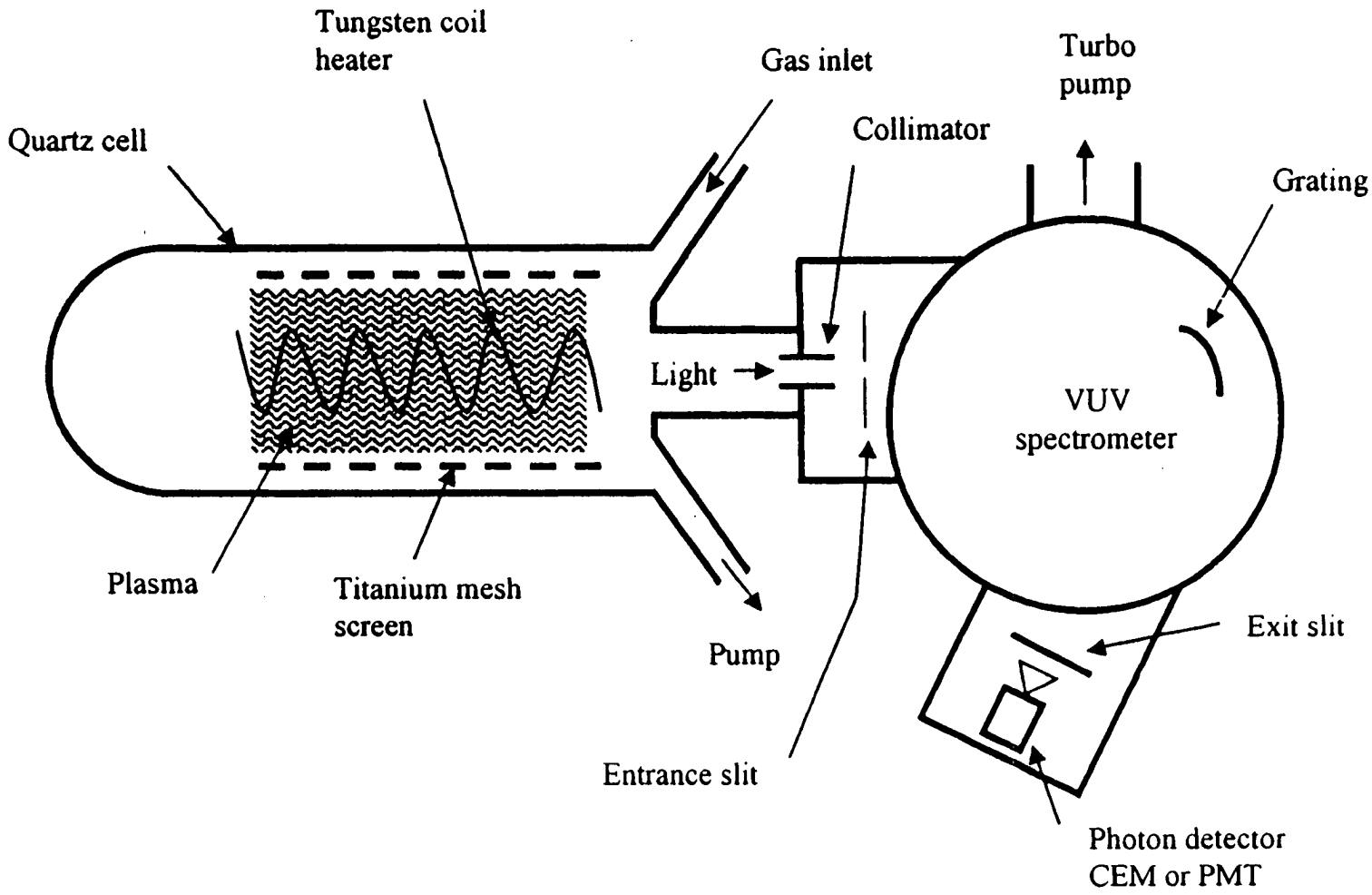
Tungsten coil heater
Gas inlet
Turbo pump
Quartz cell
Collimator
Grating
Light
VUV spectrometer
Plasma
Titanium mesh screen
Pump
Exit slit
Entrance slit
Photon detector CEM or PMT

Fig. 1

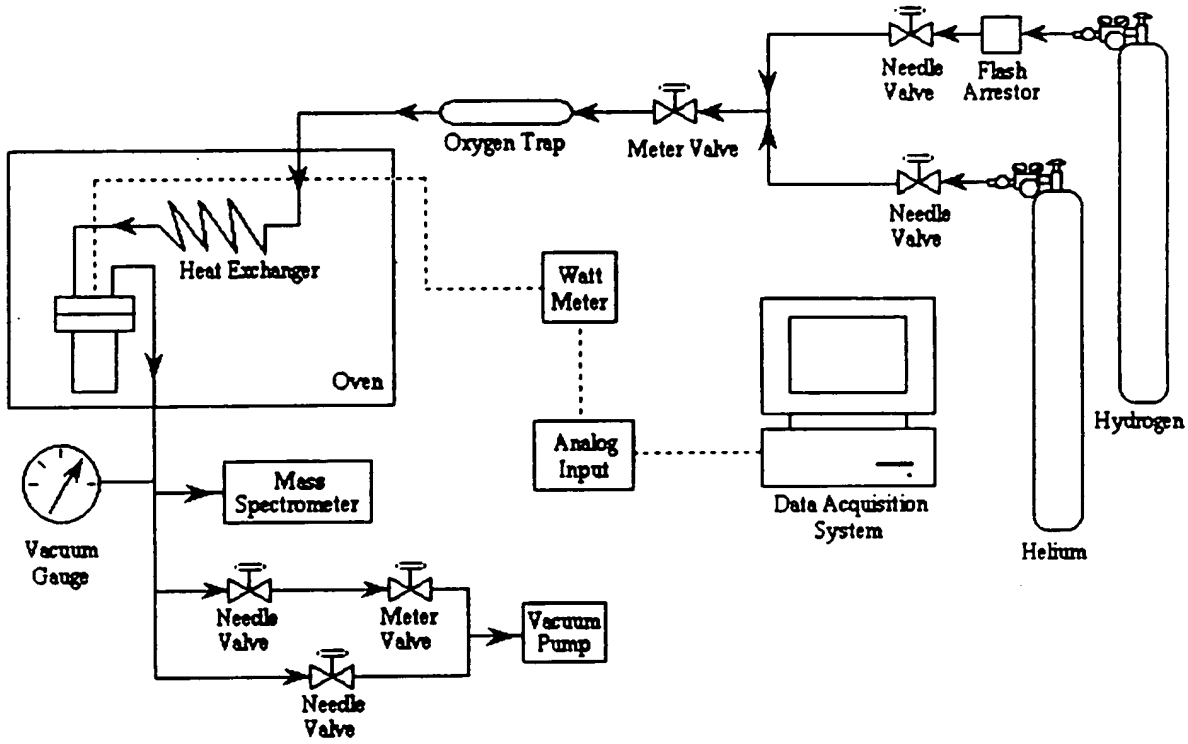
Needle Valve
Flash Arrestor
Oxygen Trap
Meter Valve
Needle Valve
Heat Exchanger
Watt Meter
Oven
Hydrogen
Analog Input
Data Acquisition System
Mass Spectrometer
Vacuum Gauge
Helium
Needle Valve
Meter Valve
Vacuum Pump
Needle Valve

Fig. 2

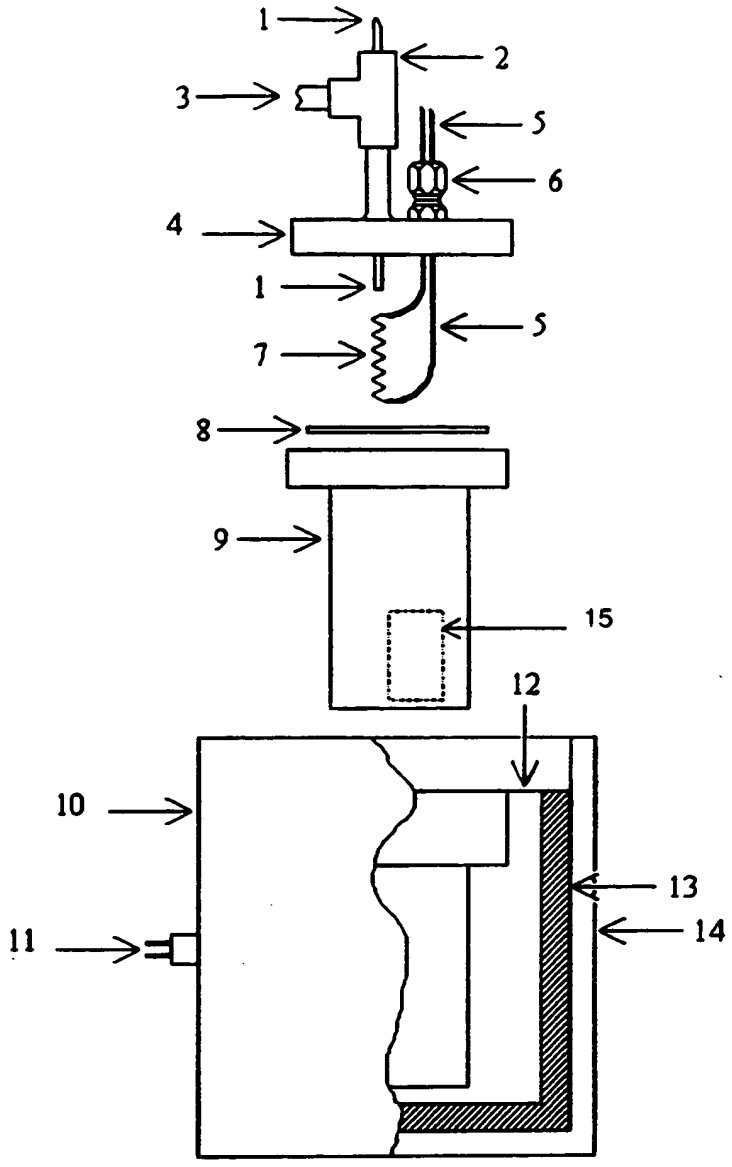

Fig. 3

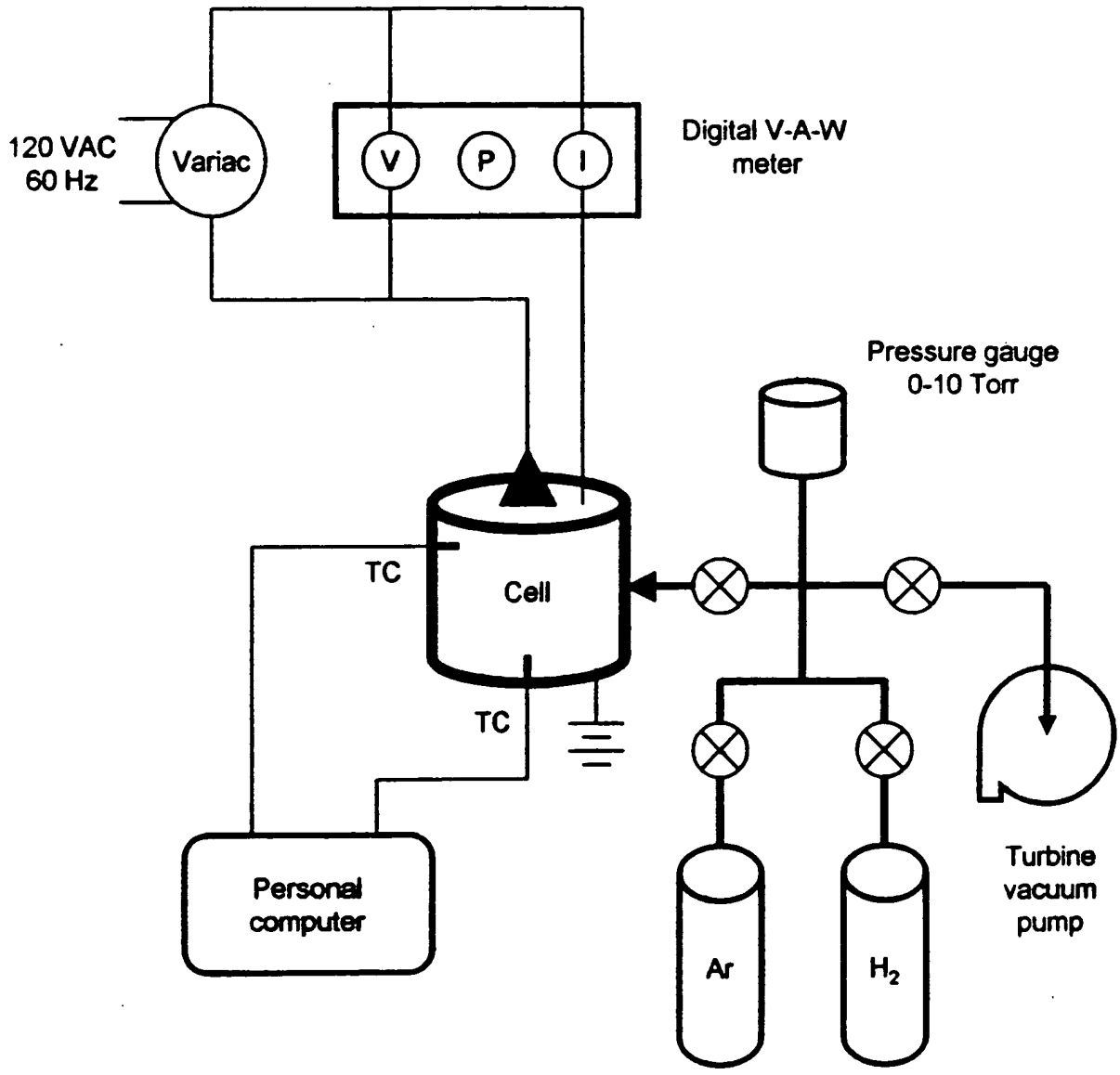
120 VAC
60 Hz
Variac
V
P
I
Digital V-A-W
meter
Pressure gauge
0-10 Torr
TC
Cell
TC
Personal
computer
Ar
H_2
Turbine
vacuum
pump

Fig. 4

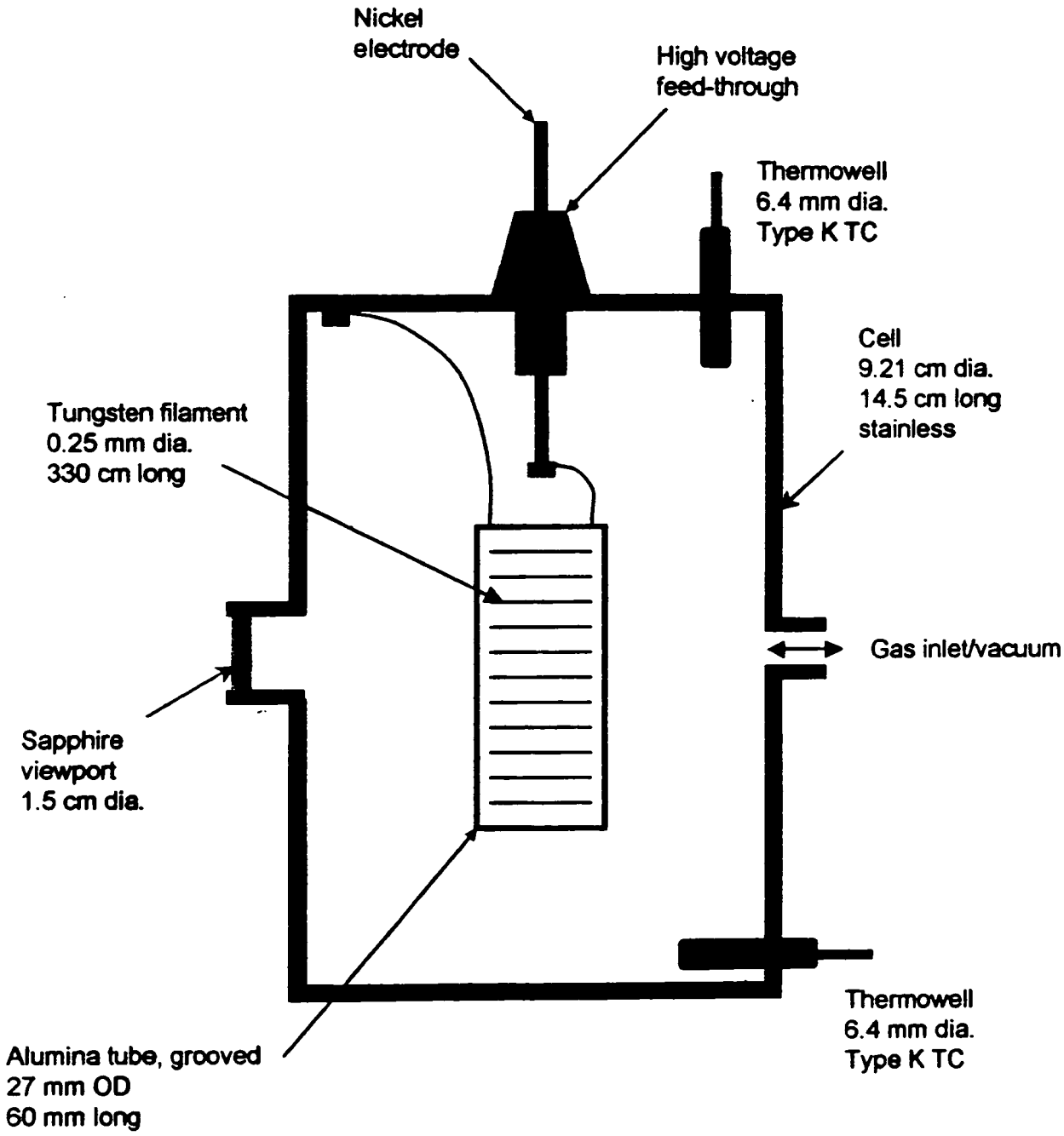
Nickel electrode
High voltage feed-through
Thermowell 6.4 mm dia. Type K TC
Cell 9.21 cm dia. 14.5 cm long stainless
Tungsten filament 0.25 mm dia. 330 cm long
Gas inlet/vacuum
Sapphire viewport 1.5 cm dia.
Thermowell 6.4 mm dia. Type K TC
Alumina tube, grooved 27 mm OD 60 mm long

Fig. 5

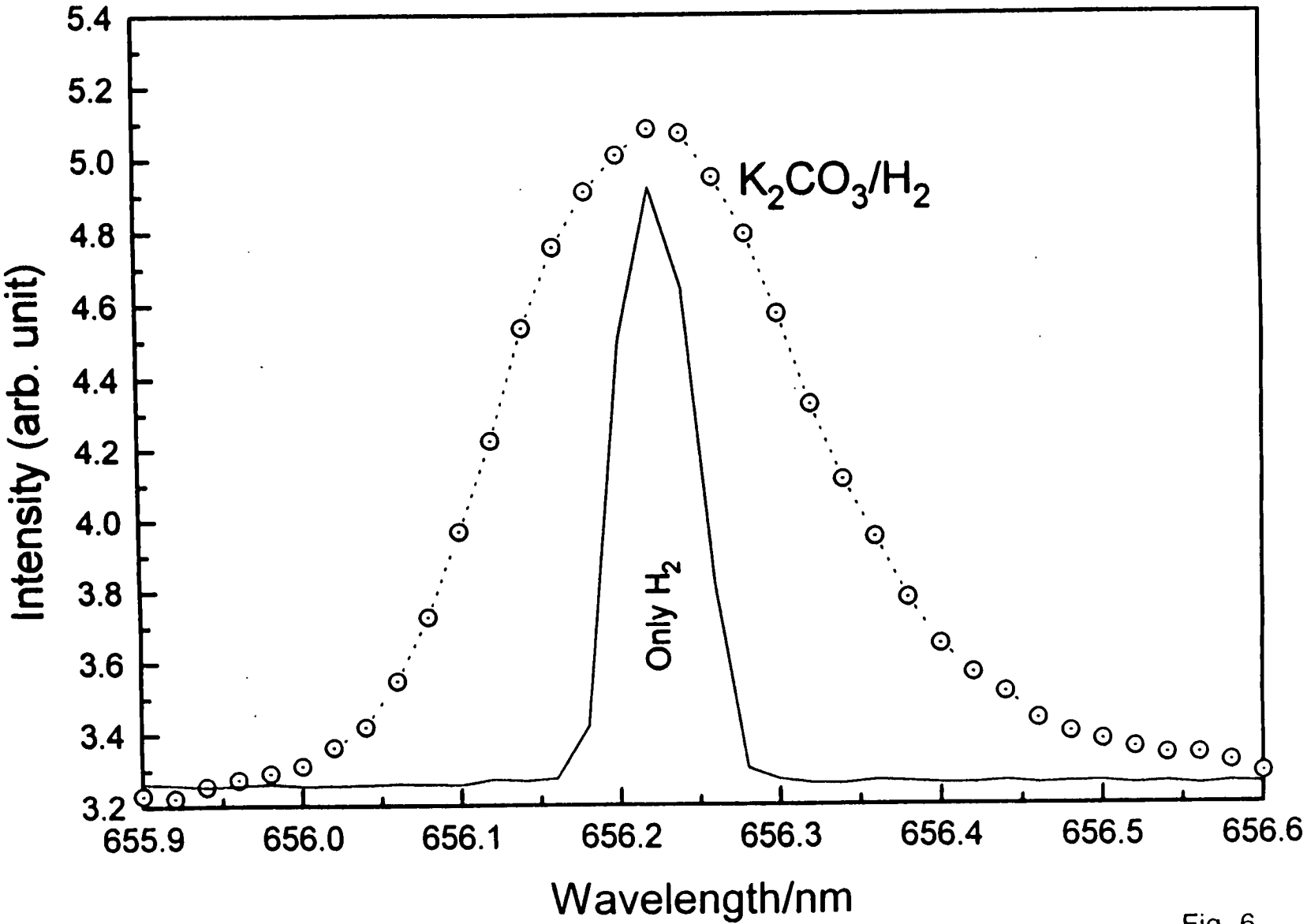
5.4
5.2
5.0
4.8
4.6
4.4
4.2
4.0
3.8
3.6
3.4
3.2
Intensity (arb. unit)
655.9
656.0
656.1
656.2
656.3
656.4
656.5
656.6
Wavelength/nm
K2CO3/H2
Only H2

Fig. 6

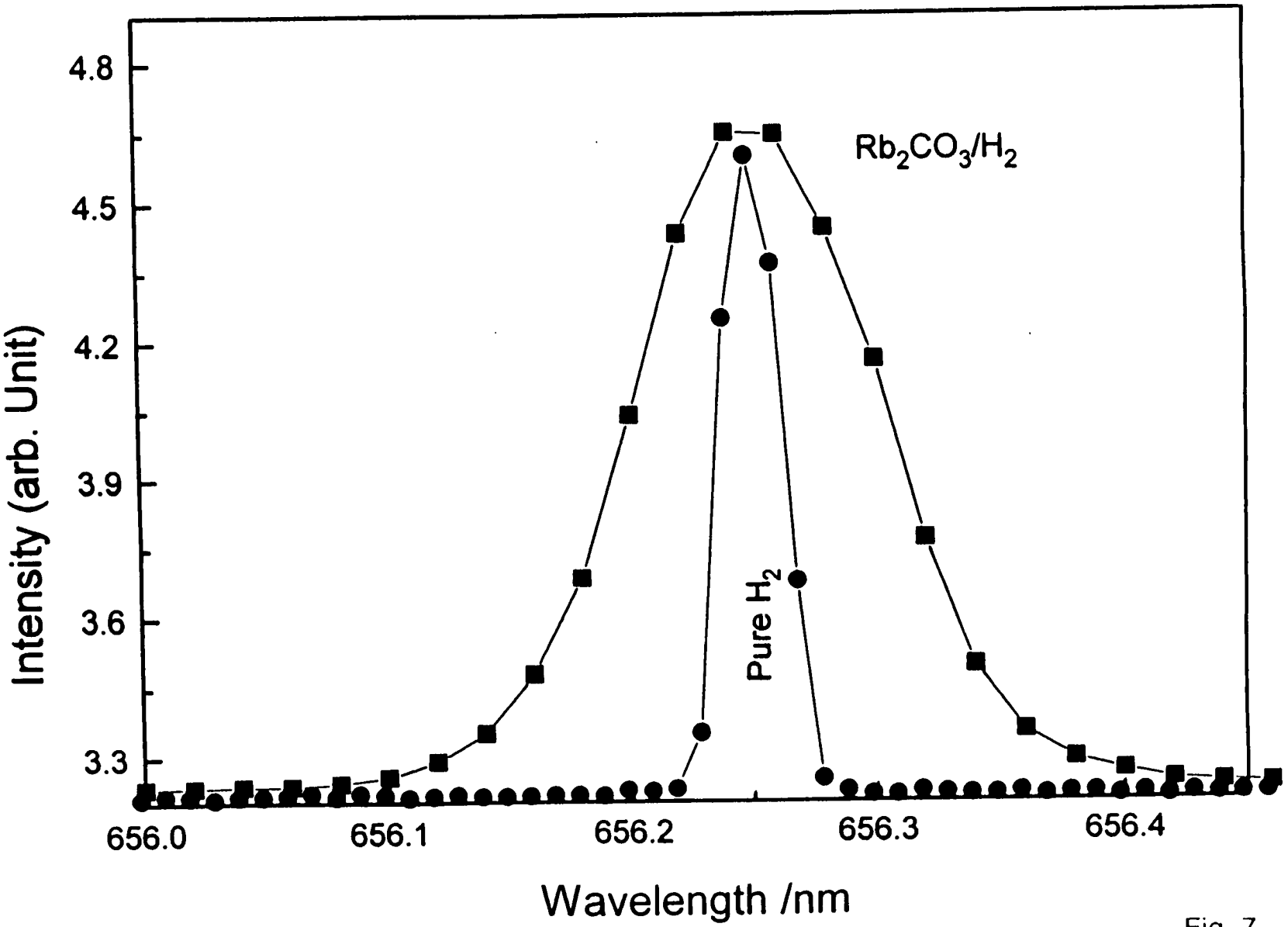
4.8
4.5
4.2
3.9
3.6
3.3
Intensity (arb. Unit)
656.0
656.1
656.2
656.3
656.4
Wavelength /nm
Rb2CO3/H2
Pure H2

Fig. 7

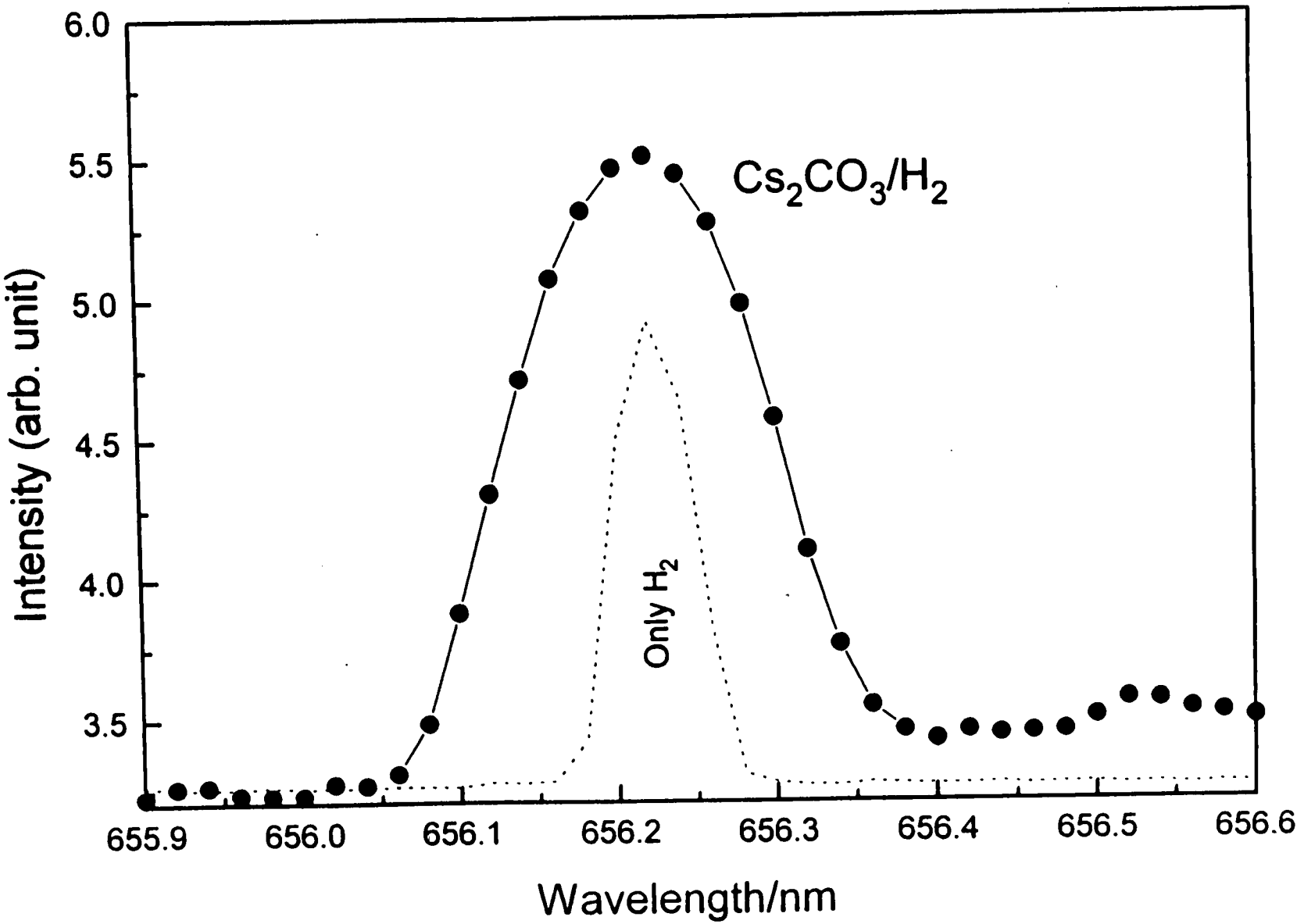
6.0
5.5
5.0
4.5
4.0
3.5
Intensity (arb. unit)
Cs_2CO_3/H_2
Only H_2
655.9
656.0
656.1
656.2
656.3
656.4
656.5
656.6
Wavelength/nm

Fig. 8

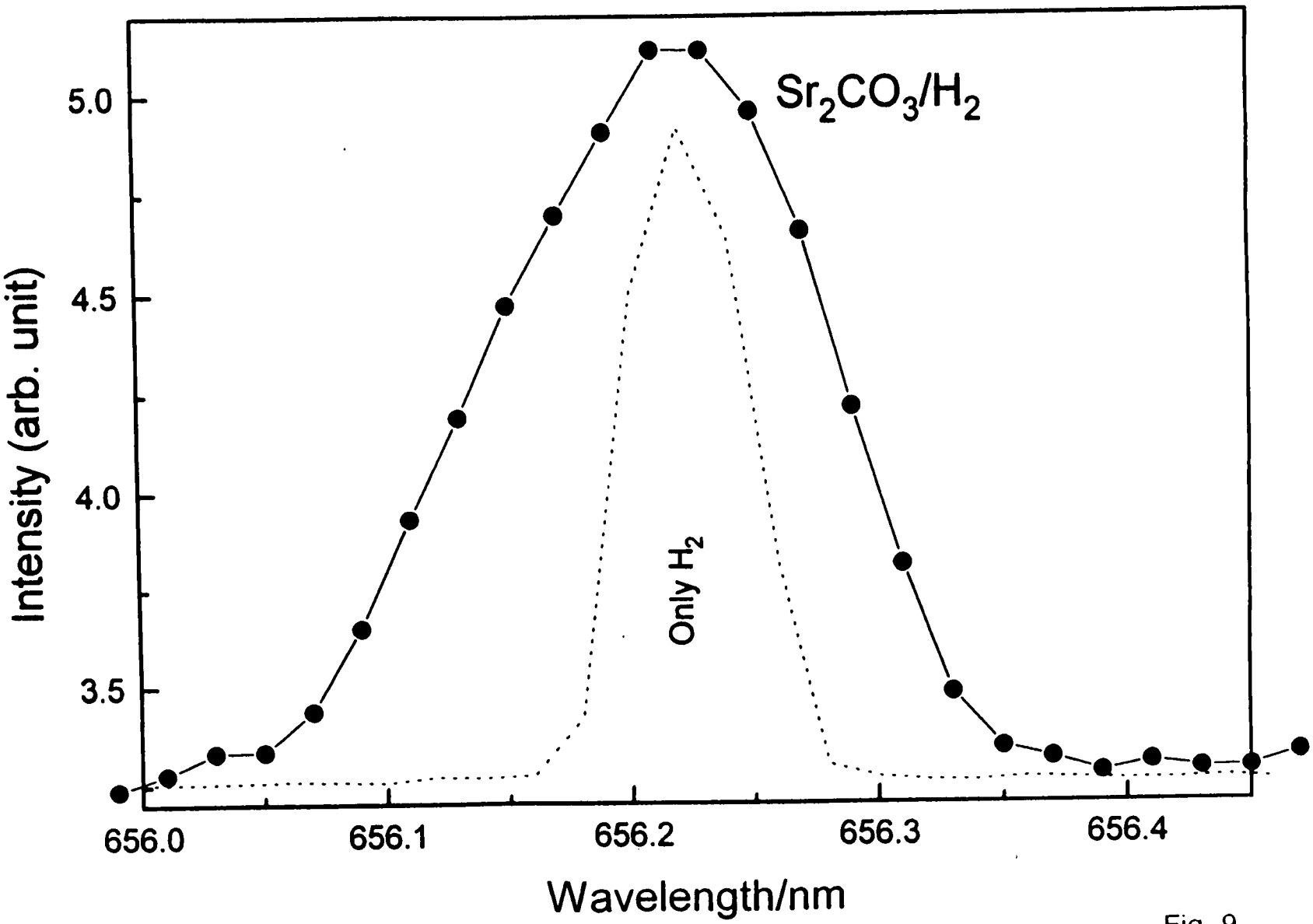
Sr2CO3/H2
Only H2
Intensity (arb. unit)
5.0
4.5
4.0
3.5
656.0
656.1
656.2
656.3
656.4
Wavelength/nm

Fig. 9

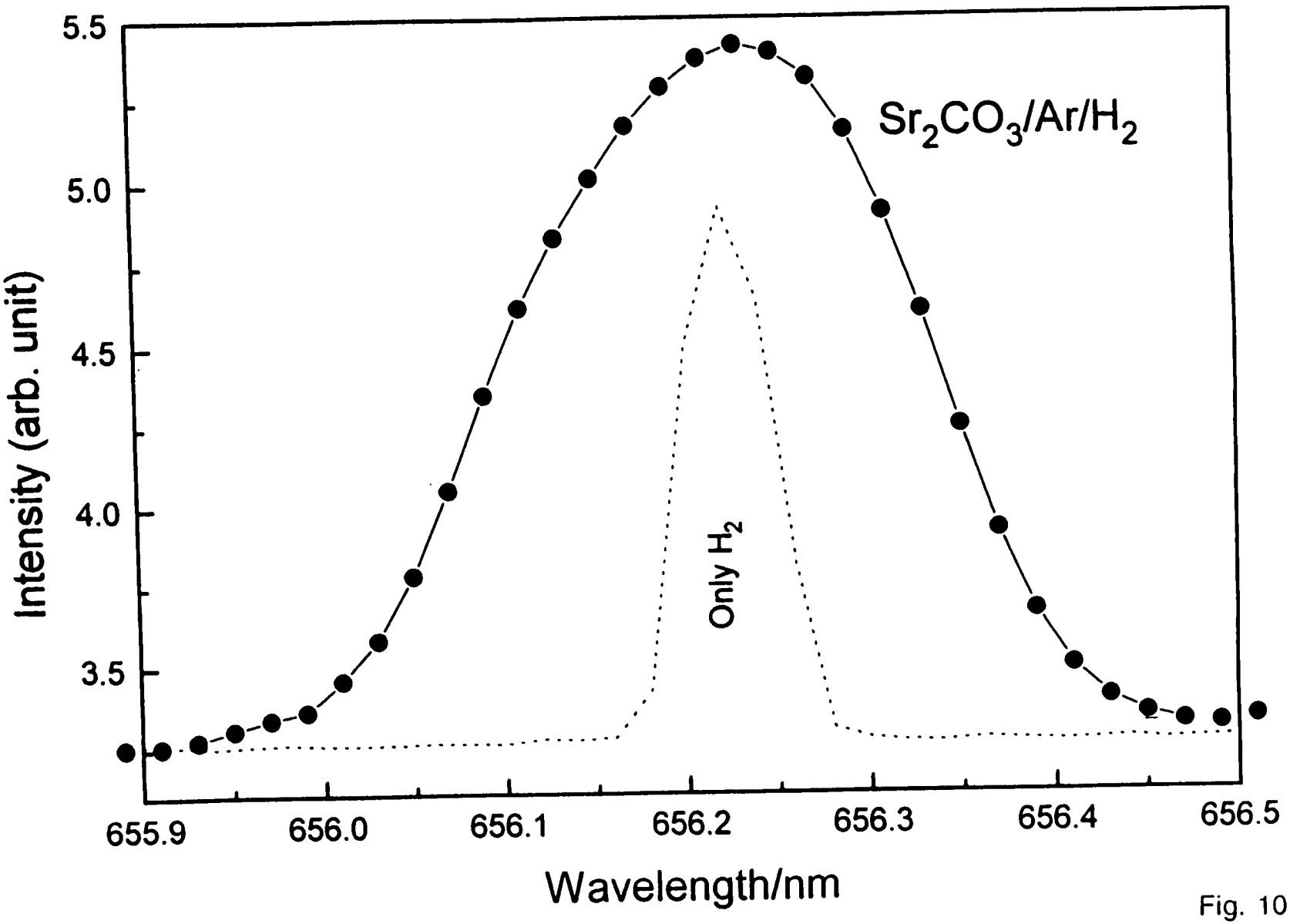
5.5
5.0
4.5
4.0
3.5
Intensity (arb. unit)
$Sr_2CO_3/Ar/H_2$
Only H_2
655.9
656.0
656.1
656.2
656.3
656.4
656.5
Wavelength/nm

Fig. 10

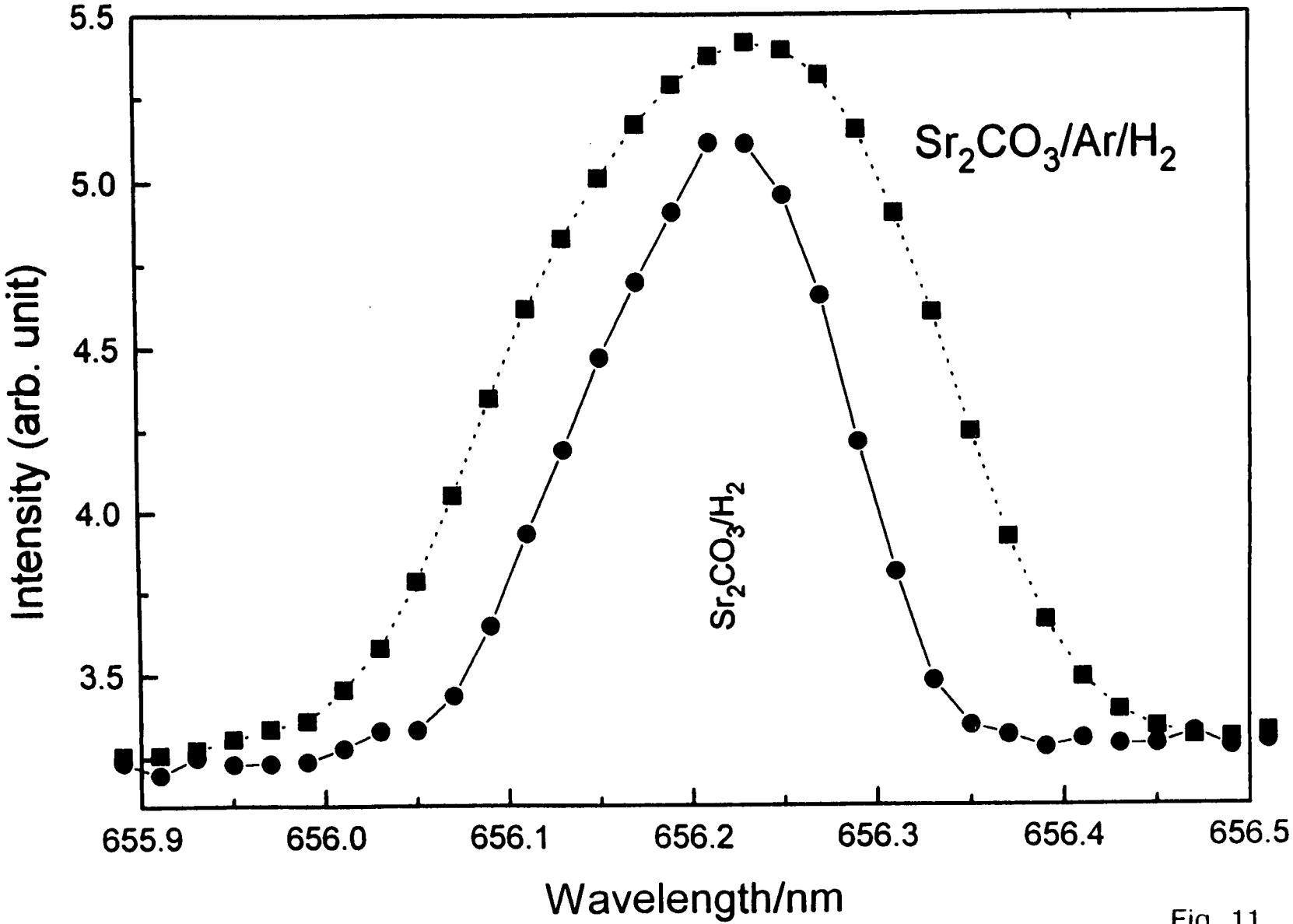
5.5
5.0
4.5
4.0
3.5
Intensity (arb. unit)
655.9
656.0
656.1
656.2
656.3
656.4
656.5
Wavelength/nm
Sr2CO3/Ar/H2
Sr2CO3/H2

Fig. 11

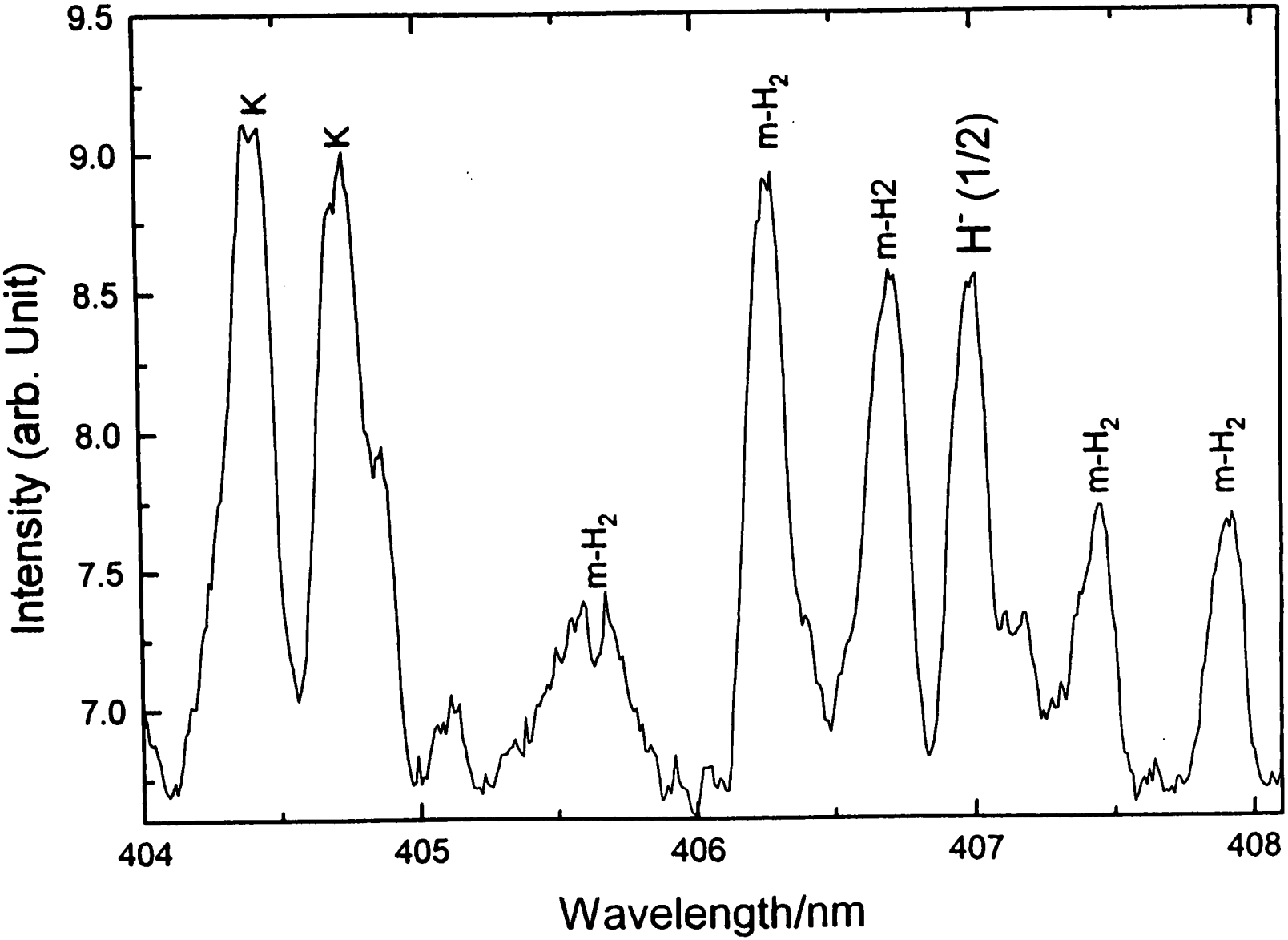
9.5
9.0
8.5
8.0
7.5
7.0
Intensity (arb. Unit)
K
K
m-H2
m-H2
H- (1/2)
m-H2
m-H2
404
405
406
407
408
Wavelength/nm

Fig. 12

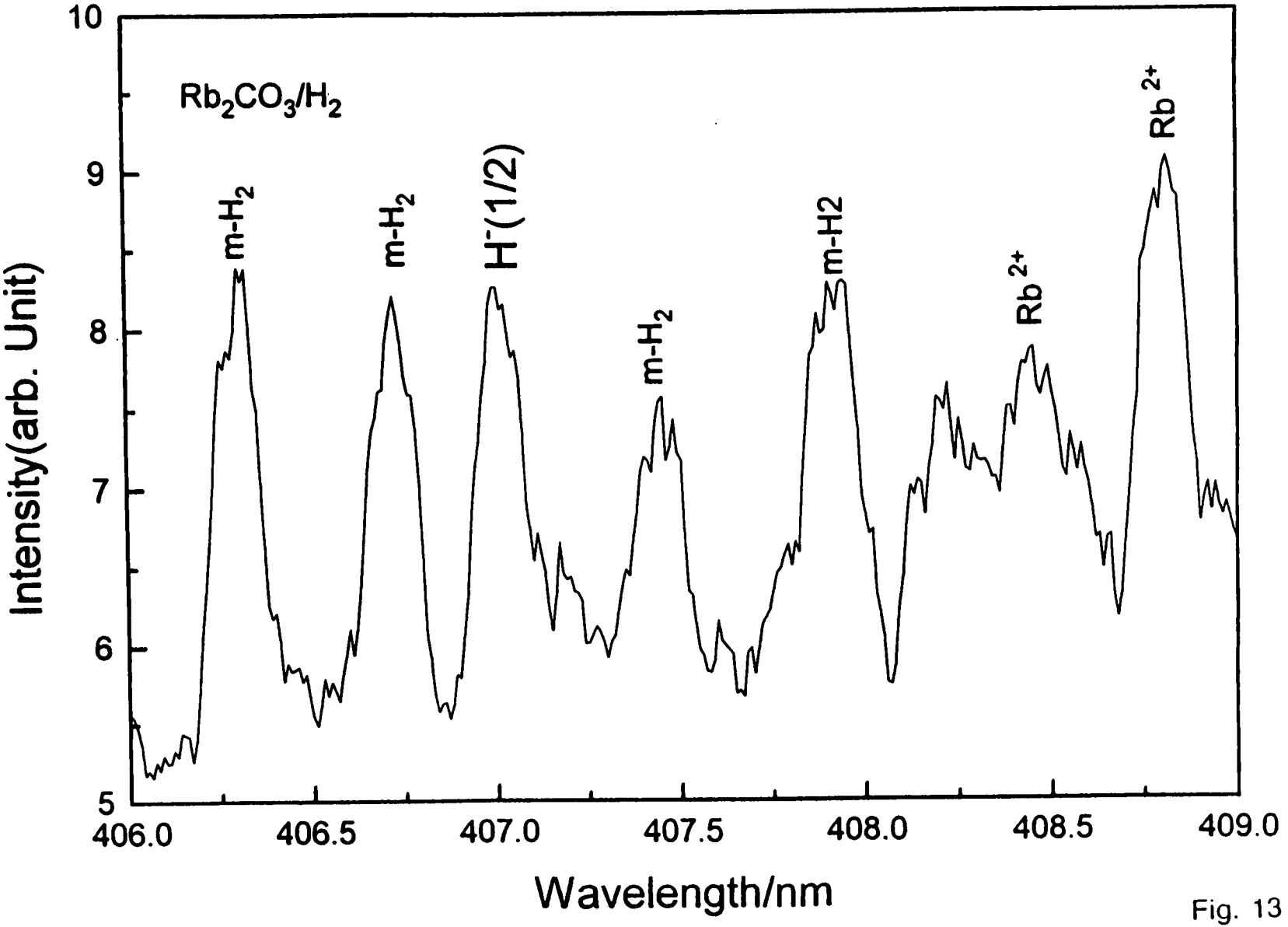
Rb2CO3/H2
m-H2
m-H2
H-(1/2)
m-H2
m-H2
Rb 2+
Rb 2+
Intensity(arb. Unit)
Wavelength/nm
10
9
8
7
6
5
406.0
406.5
407.0
407.5
408.0
408.5
409.0

Fig. 13

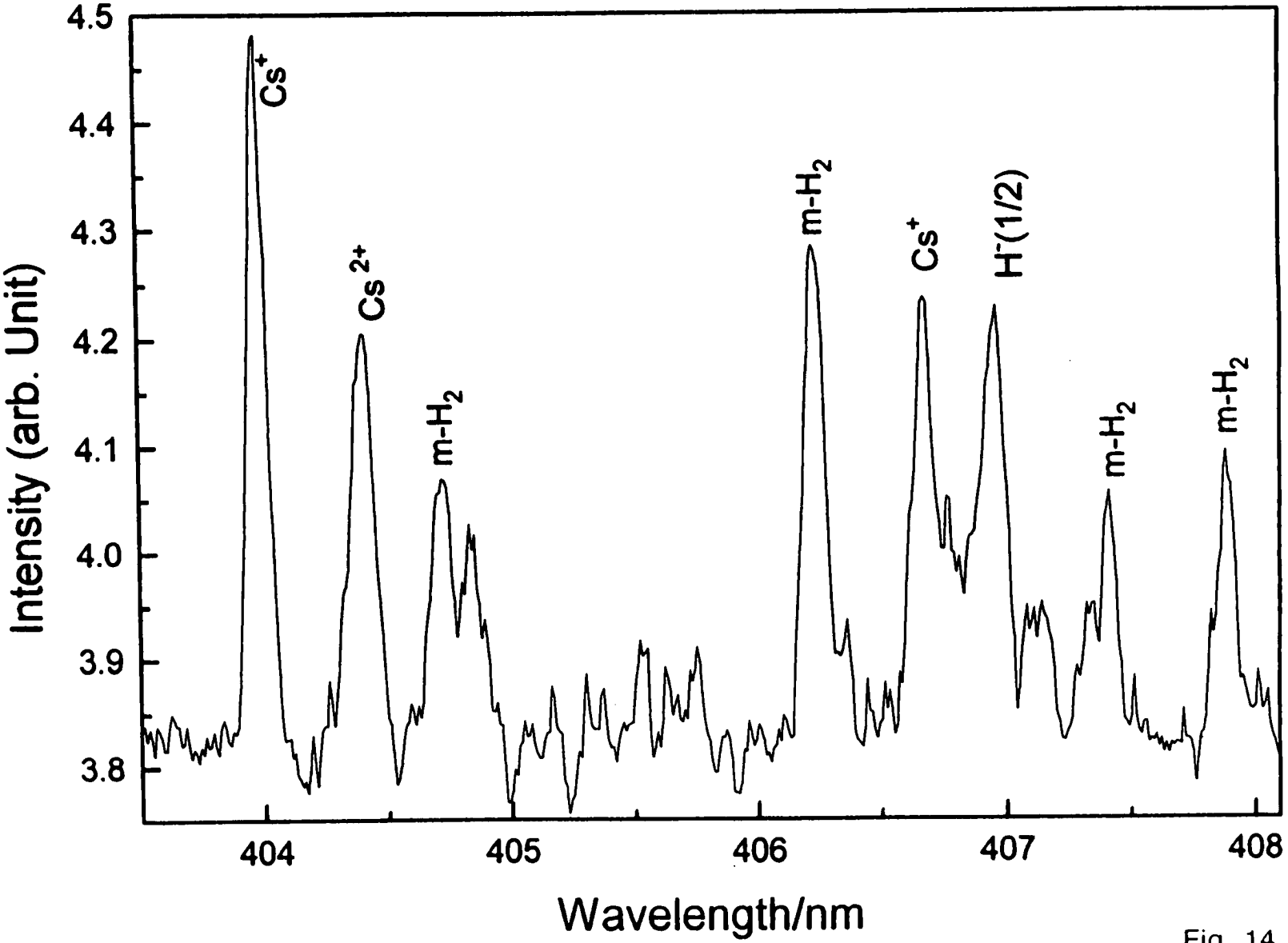
Intensity (arb. Unit)
4.5
4.4
4.3
4.2
4.1
4.0
3.9
3.8
404
405
406
407
408
Wavelength/nm
Cs+
Cs2+
m-H2
m-H2
Cs+
H-(1/2)
m-H2
m-H2

Fig. 14

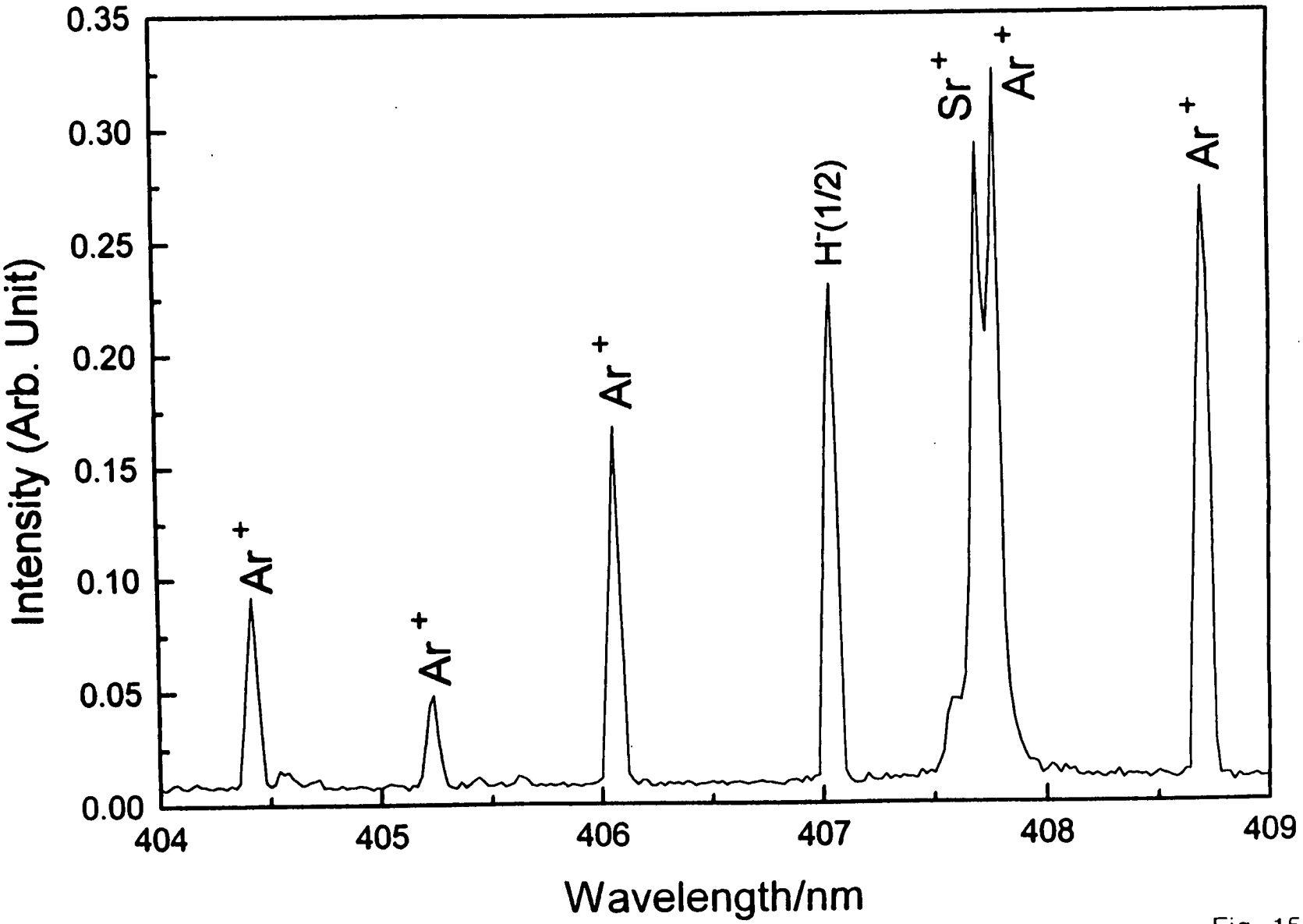
0.35
0.30
0.25
0.20
0.15
0.10
0.05
0.00
Intensity (Arb. Unit)
404
405
406
407
408
409
Wavelength/nm
Ar+
Ar+
Ar+
H-(1/2)
Sr+
Ar+
Ar+

Fig. 15

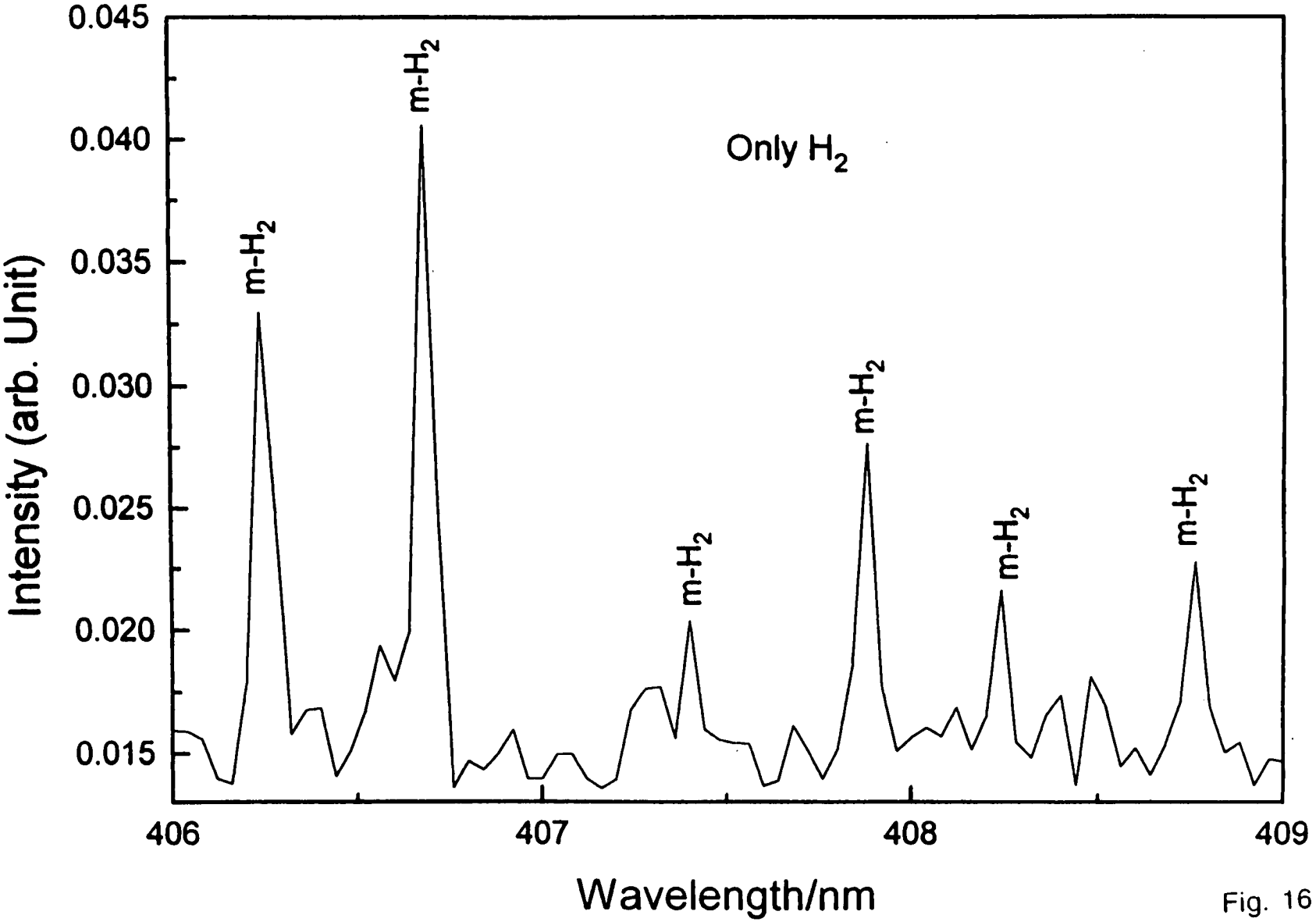
0.045
0.040
0.035
0.030
0.025
0.020
0.015
Intensity (arb. Unit)
406
407
408
409
Wavelength/nm
Only H_2
m-H_2
m-H_2
m-H_2
m-H_2
m-H_2
m-H_2

Fig. 16

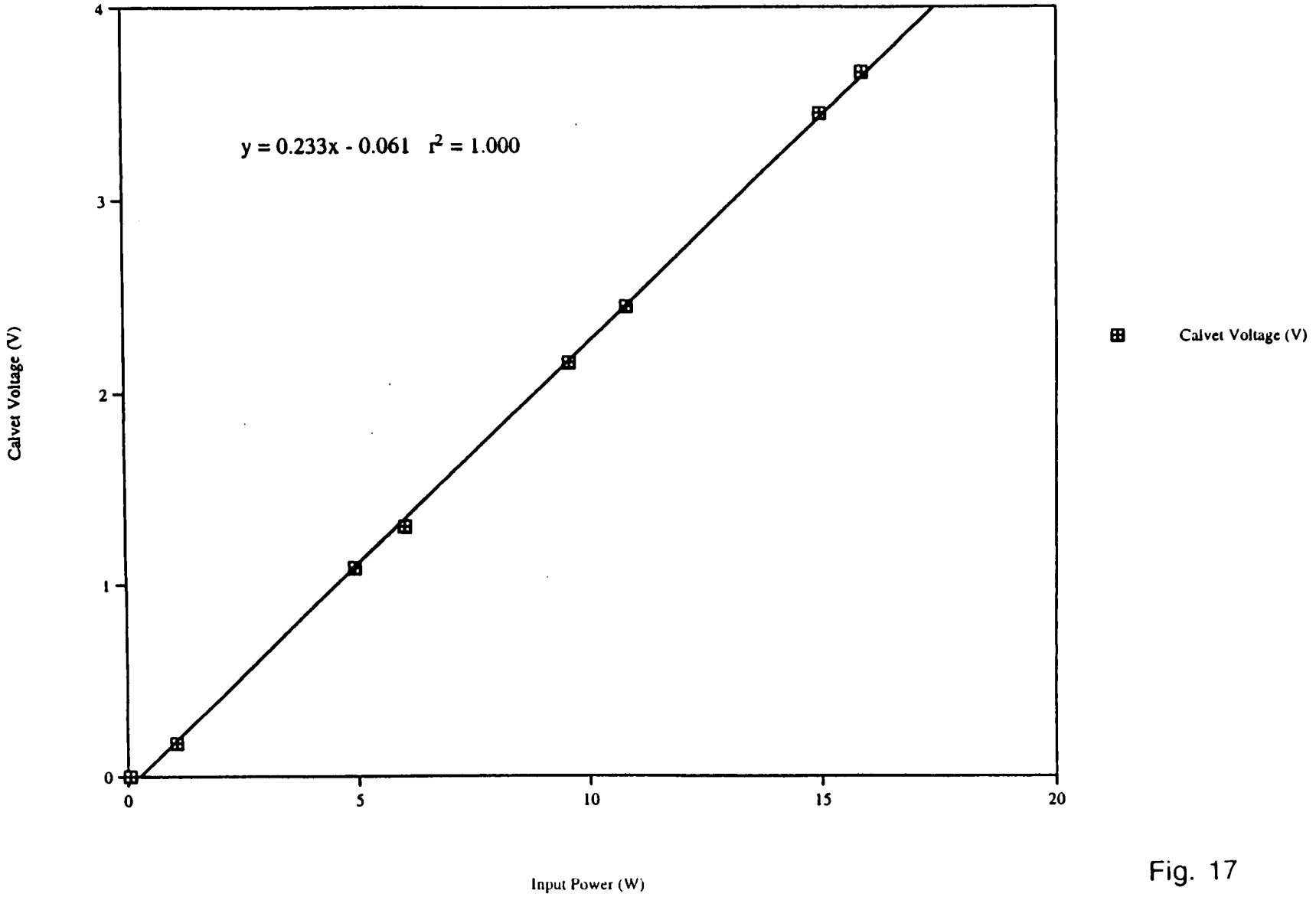
y = 0.233x - 0.061 r² = 1.000
Calvet Voltage (V)
Input Power (W)
0
1
2
3
4
0
5
10
15
20
Calvet Voltage (V)

Fig. 17

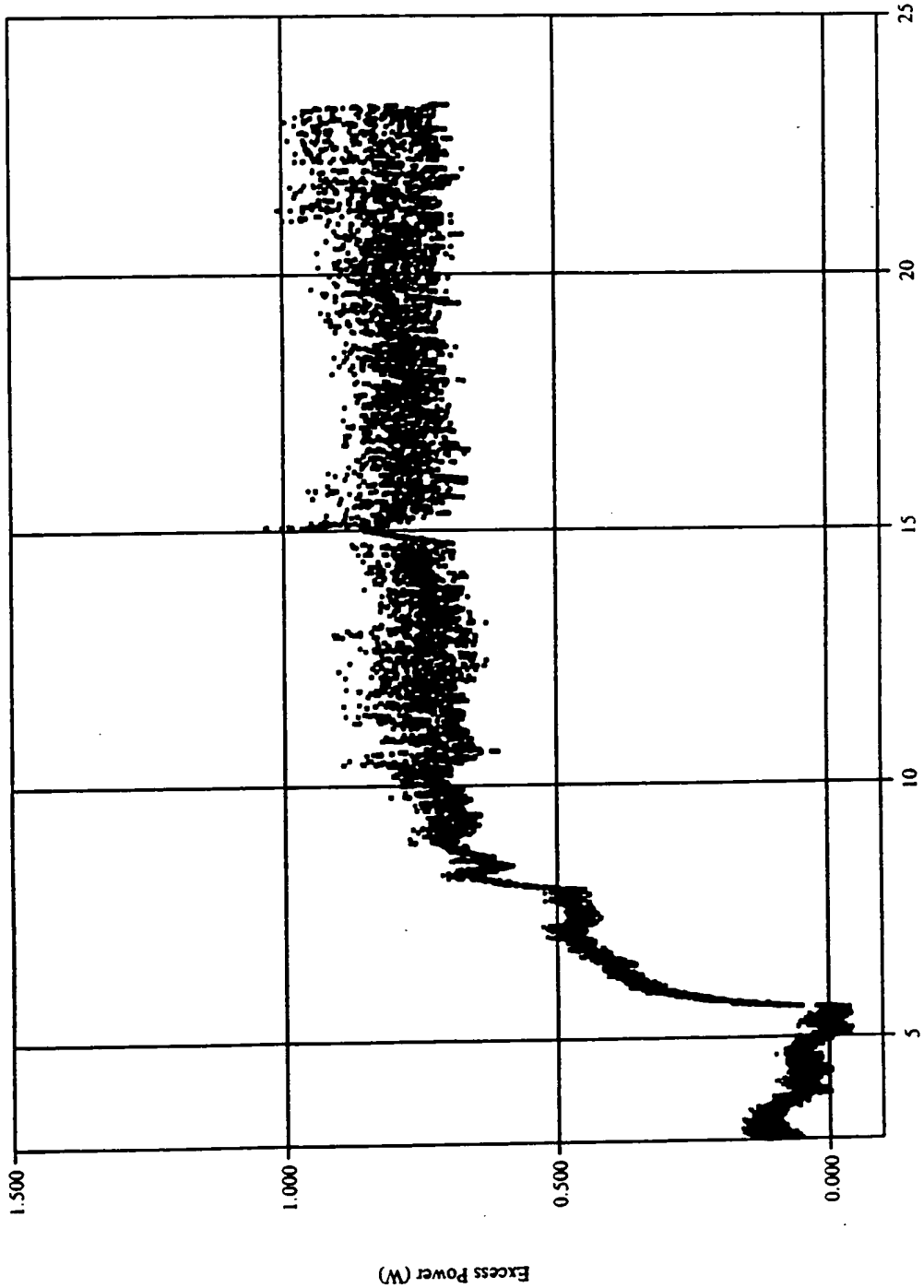

Fig. 18

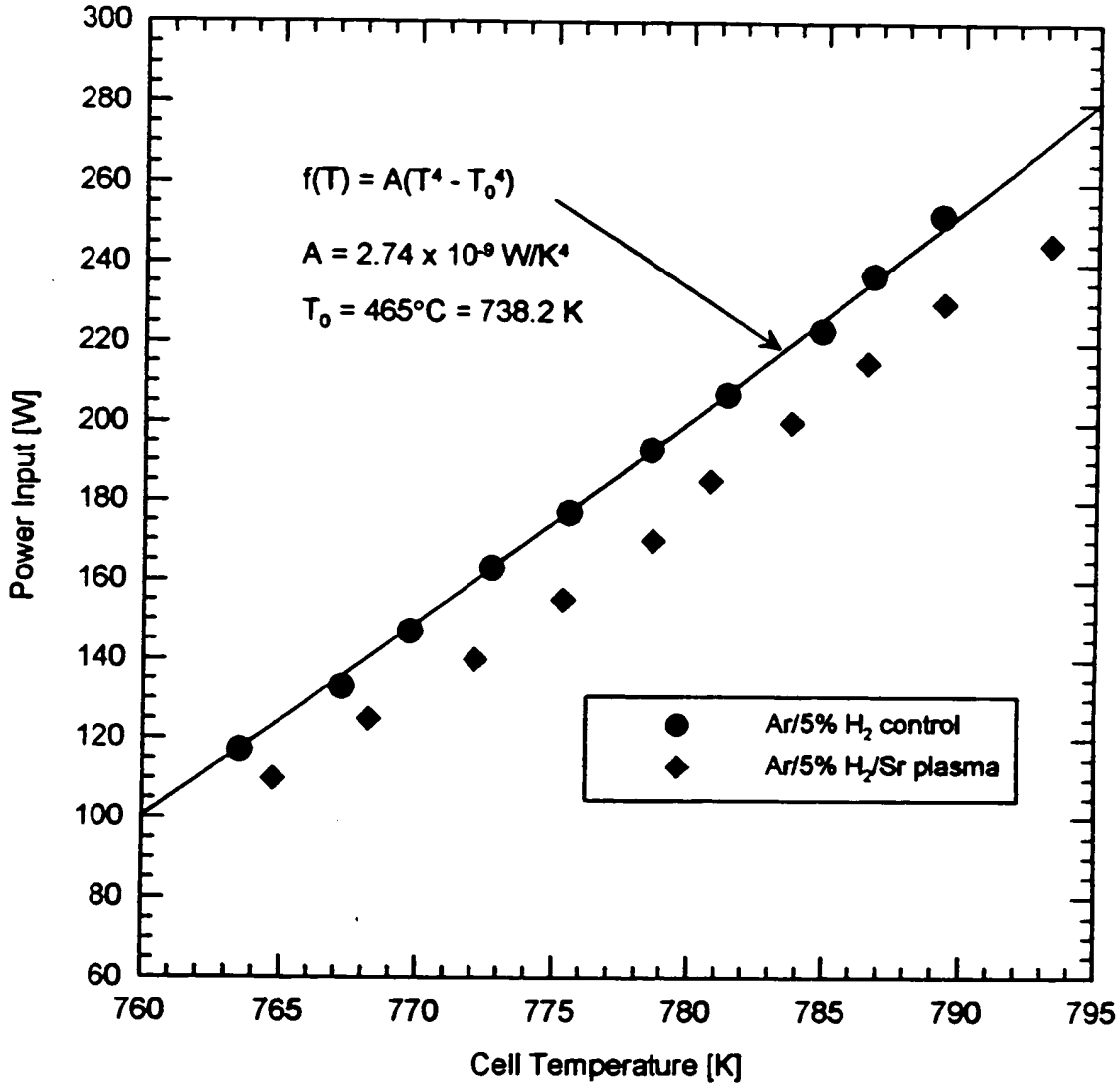
300
280
260
240
220
200
180
160
140
120
100
80
60
760
765
770
775
780
785
790
795
Power Input [W]
Cell Temperature [K]
f(T) = A(T⁴ - T₀⁴)
A = 2.74 x 10⁻⁹ W/K⁴
T₀ = 465°C = 738.2 K
Ar/5% H₂ control
Ar/5% H₂/Sr plasma

Fig. 19